

**Nagra**

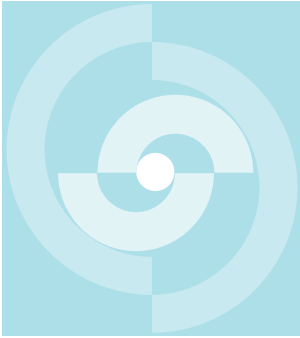
Nationale  
Genossenschaft  
für die Lagerung  
radioaktiver Abfälle

**Cédra**

Société coopérative  
nationale  
pour l'entreposage  
de déchets radioactifs

**Cisra**

Società cooperativa  
nazionale  
per l'immagazzinamento  
di scorie radioattive



# TECHNICAL REPORT 89-15

GRIMSEL TEST SITE

## HYDROGEOLOGICAL CHARACTERISATION OF THE MIGRATION EXPERIMENTAL AREA AT THE GRIMSEL TEST SITE

E. HOEHN  
TH. FIERZ  
P. THORNE

JULY 1990

PSI, Würenlingen and Villigen

GRIMSEL TEST SITE / SWITZERLAND  
A JOINT RESEARCH PROGRAM BY

- NAGRA – National Cooperative for the Storage of Radioactive Waste, Baden, Switzerland
- BGR — Federal Institute for Geoscience and Natural Resources, Hannover, Federal Republic of Germany
- GSF — Research Centre for Environmental Sciences, Munich, Federal Republic of Germany



**Nagra**

Nationale  
Genossenschaft  
für die Lagerung  
radioaktiver Abfälle

**Cédra**

Société coopérative  
nationale  
pour l'entreposage  
de déchets radioactifs

**Cisra**

Società cooperativa  
nazionale  
per l'immagazzinamento  
di scorie radioattive

# TECHNICAL REPORT 89-15

GRIMSEL TEST SITE

## HYDROGEOLOGICAL CHARACTERISATION OF THE MIGRATION EXPERIMENTAL AREA AT THE GRIMSEL TEST SITE

E. HOEHN  
TH. FIERZ  
P. THORNE

JULY 1990

PSI, Würenlingen and Villigen

GRIMSEL TEST SITE / SWITZERLAND  
A JOINT RESEARCH PROGRAM BY

- NAGRA - National Cooperative for the Storage of Radioactive Waste, Baden, Switzerland
- BGR — Federal Institute for Geoscience and Natural Resources, Hannover, Federal Republic of Germany
- GSF — Research Centre for Environmental Sciences, Munich, Federal Republic of Germany



## FOREWORD

Concepts which foresee the disposal of radioactive waste in geological formations lay great weight on acquiring knowledge of the proposed host rock and the surrounding rock strata. For this reason, Nagra has, since May 1984, been operating the Grimsel Test Site which is situated at a depth of 450 m in the crystalline formation of the Aar Massif. The general objectives of the research being carried out in this system of test tunnels include, in particular

- the build-up of know-how in planning, performing and interpreting underground experiments in different scientific fields and
- the acquisition of practical experience in developing, testing and applying test equipment and measuring techniques.

The Test Site (GTS) is operated by Nagra. On the basis of a German-Swiss cooperation agreement, the various experiments are carried out by Nagra, the Federal Institute for Geoscience and Natural Resources (BGR) and the Research Centre for Environmental Sciences (GSF); the latter two bodies are supported in this venture by the German Federal Ministry for Research and Technology (BMFT).

NTB 85-47 gives an overview of the GTS and a review of the status of the investigation programme as at August 1985.

This report was produced in accordance with the cooperation agreement between the three partners mentioned previously. The authors have presented their own opinions and conclusions, which do not necessarily coincide with those of Nagra, BGR or GSF.



## GRIMSEL-GEBIET

Blick nach Westen

- 1 Felslabor
- 2 Juchlistock
- 3 Räterichsbodensee
- 4 Grimselsee
- 5 Rhonetal

## GRIMSEL AREA

View looking West

- 1 Test Site
- 2 Juchlistock
- 3 Lake Raeterichsboden
- 4 Lake Grimsel
- 5 Rhone Valley

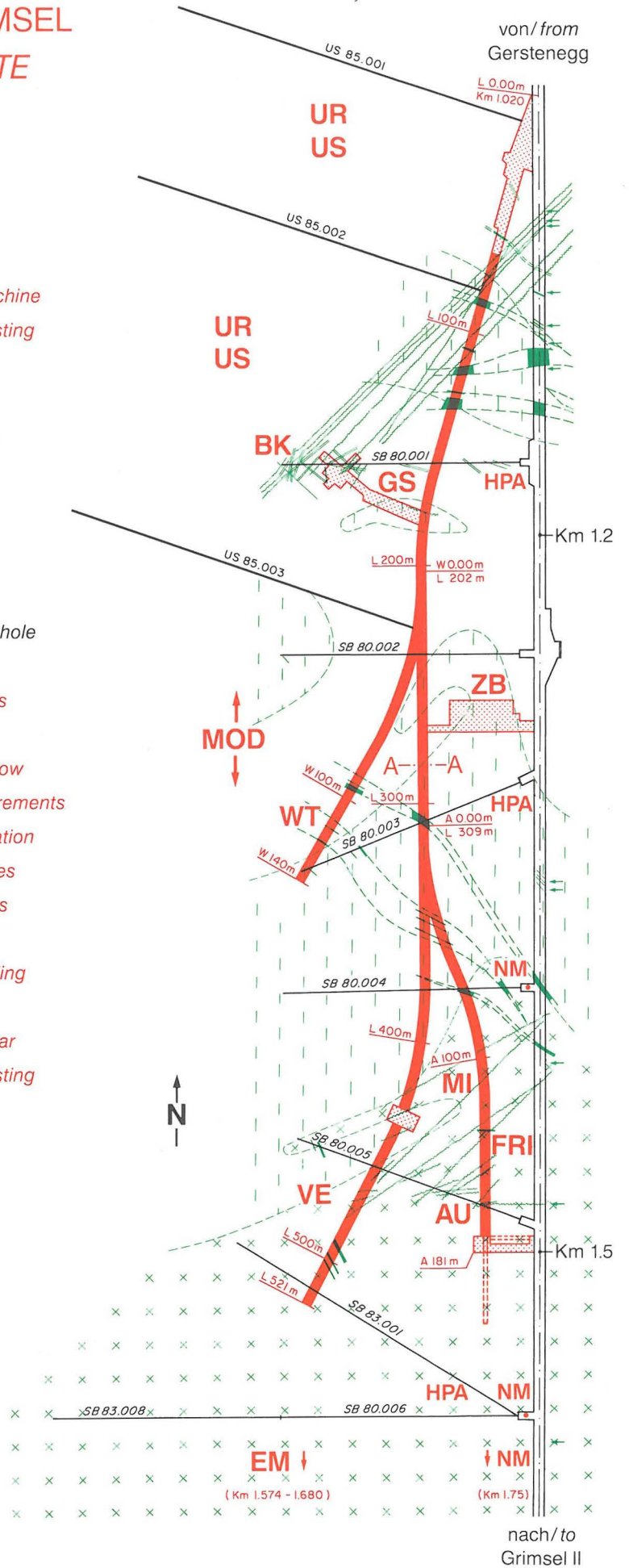
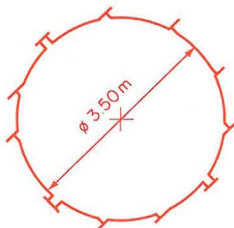
**FLG** FELSLABOR GRIMSEL  
**GTS** GRIMSEL TEST SITE

Situation



- Zugangsstollen/ Access tunnel
- Fräsvortrieb/ by tunnel boring machine
- Sprengvortrieb/ excavated by blasting
- Zentraler Aaregranit ZAGR  
Central Aaregranite CAGR
- Biotitreicher ZAGR  
CAGR with high content of biotite
- Grimsel-Granodiorit  
Grimsel-Granodiorite
- Scherzone/ Shear zone
- Lamprophyre/ Lamprophyre
- Wasserzutritt/ Water inflow
- Sondierbohrung/ Exploratory borehole
- US Bohrung/ US borehole
- ZB** Zentraler Bereich/ Central facilities
- AU** Auflockerung/ Excavation effects
- BK** Bohrlochkranz/ Fracture system flow
- EM** El.magn. HF-Messungen/ -measurements
- FRI** Kluftzone/ Fracture zone investigation
- GS** Gebirgsspannungen/ Rock stresses
- HPA** Hydr. Parameter/ Hydr. parameters
- MI** Migration/ Migration
- MOD** Hydrodyn. Modellierung/ H. modeling
- NM** Neigungsmesser/ Tiltmeters
- UR** Untertageradar/ Underground radar
- US** Seismik/ Underground seismic testing
- VE** Ventilationstest/ Ventilation test
- WT** Wärmeversuch/ Heat test

A — A Schnitt/ Section



## **Preface**

In the framework of its Waste Management Programme the Paul Scherrer Institute is performing work to increase the understanding of the geochemistry of nuclear waste relevant radionuclides. These investigations are performed in close cooperation with, and with the financial support of NAGRA. The present report is issued simultaneously as a PSI report and a NAGRA NTB.

# Contents

<b>Abstract</b>	<b>1</b>
<b>Zusammenfassung</b>	<b>2</b>
<b>Résumé</b>	<b>3</b>
<b>1 Introduction</b>	<b>4</b>
<b>2 Site Selection</b>	<b>6</b>
<b>3 Site Instrumentation and Exploration with Boreholes</b>	<b>10</b>
3.1 Instrumentation at the Tunnel Wall . . . . .	10
3.2 Exploration With Boreholes . . . . .	10
3.3 Borehole Instrumentation . . . . .	17
<b>4 Flow Field</b>	<b>19</b>
4.1 Discharge From the Migration Fracture to the Tunnel . . . . .	19
4.2 Hydraulic Pressure in Boreholes . . . . .	21
<b>5 Hydraulic Tests in Boreholes</b>	<b>27</b>
5.1 Preliminary Pulse Tests . . . . .	27
5.2 Methods for Hydraulic Test Analysis . . . . .	27
5.3 Evaluation of Constant–Drawdown Tests . . . . .	30
5.4 Evaluation of Constant–Discharge Tests . . . . .	37
5.5 Discussion of Constant–Drawdown and Constant–Discharge Tests . . . . .	38
5.6 Long–Term, Constant–Discharge Test of Borehole BOMI 87.009 . . . . .	40
<b>6 Conclusions</b>	<b>44</b>

<b>Acknowledgement</b>	<b>45</b>
<b>References</b>	<b>46</b>
<b>Appendix A: Supplement to the chemical characterisation of the groundwaters</b>	<b>50</b>
<b>Appendix B: Compilation of Transmissivity and Storage-Coefficient Calculations</b>	<b>56</b>

## Abstract

Tracer migration experiments in a single fracture in granodioritic rock are in progress at the underground Grimsel Test Site (GTS), to test radionuclide transport models and to develop experimental techniques. This report recapitulates the exploration of the site and provides information on the instrumentation of the location chosen for migration experiments.

Preliminary estimations of groundwater flow velocities into the tunnel in four different fracture zones (lamprophyre dikes, and mylonitic zones) led to a selection of a location (at AU96m, GTS metering) considered optimally suited for migration experiments. The hydrogeology of the chosen single (proto)mylonitic fracture was unknown at the scale of about 10 x 10 m and had to be explored with boreholes. Ten boreholes proved that the fracture is an almost planar element in the water-saturated rock mass. Eight boreholes yield sufficient groundwater for the measurement of hydraulic pressure and for groundwater sampling. Most boreholes are equipped with a system of triple packers which isolate the fracture and the borehole mouth. Passive hydraulic tests proved that a hydraulic connection exists between the boreholes and that the transmissivity of the fracture is about 0.6 m<sup>2</sup>/d. Long-term monitoring revealed a decline of hydraulic pressure of about 0.08 bar/y, which indicates that the hydraulic system has not yet fully reached a steady state.

Plastic sheets mounted on the wall of the tunnel at its intersection with the fracture allow the measurement of the discharge of groundwater, which is in the order of 0.5 L/min at the migration location. From the observation of breakthrough phenomena during drilling of boreholes and the miscible displacement of groundwaters of a slightly different composition during injection-extraction experiments, a flow velocity at the migration location was estimated to be in the order of a few meters per hour. The groundwater does not contain tritium in detectable amounts and, therefore, the reservoir volume of groundwater, which discharges to the tunnel, must be high (i.e. more than 200 m<sup>3</sup>). The fracture of interest is probably hydraulically connected to a major shear zone in the area.

## Zusammenfassung

Im Felslabor Grimsel sind in einer Einzelkluft in granodioritischem Gestein Markierversuche im Gange, um Modelle des Radionuklid-Transports zu eichen und experimentelle Techniken zu entwickeln. Dieser Bericht umfasst die Geschichte der Suche nach einem geeigneten Ort für Markierversuche und macht Angaben über die Ausrüstung dieses Versuchsorts.

Erste Abschätzungen über Fliessgeschwindigkeiten des Grundwassers in den Stollen, welche an vier verschiedenen Stellen des Felslabors mit Klüften (Lamprophyr-Gänge und Mylonitzonen) durchgeführt wurden, führte zur Auswahl eines Versuchsorts (AU96m), der in der Folge als am besten geeignet betrachtet wurde. Die hydrogeologischen Verhältnisse dieser mylonitischen Einzelkluft im Massstab von etwa 10 mal 10 Metern waren aber unbekannt und mussten daher mit Bohrungen erkundet werden. Zehn abgeteufte Bohrlöcher bewiesen, dass die Kluft ein nahezu planares Element im wassergesättigten Felsmassiv darstellt. Acht dieser Bohrlöcher führen genügend Grundwasser, um eine Messung des hydraulischen Drucks und eine Probenahme zu erlauben. Die meisten Bohrungen sind mit einem System von drei wassergefüllten Packern ausgerüstet, welche die Kluft und den Bohrloch-Mund isolieren. Passive hydraulische Tests (Auslauf-Versuche) zeigten, dass die Grundwässer in den Bohrlöchern kommunizieren. Eine Transmissibilität der Kluft wurde zu ca.  $0.6 \text{ m}^2/\text{d}$  abgeschätzt. Die Langzeit-Überwachung zeigt ein Sinken des hydraulischen Drucks von etwa 0.08 bar pro Jahr, was beweist, dass das hydraulische System im Fels noch keinen stationären Zustand erreicht hat.

Plastic-Folien, welche an die Stollenwand an ihrer Schnittstelle mit der Kluft angebracht wurden, erlauben eine Messung der Schüttung von Grundwasser. An der ausgewählten Stelle liegt diese im Bereich von 0.5 L/min. Aus der Beobachtung von Durchbruch-Phänomenen während des Bohrens und anlässlich von Experimenten, während welcher das Grundwasser durch eines von leicht verschiedener Beschaffenheit ausgetauscht wurde, konnte eine Fliessgeschwindigkeit des Grundwassers am Versuchsort Migration von etwa einigen Metern pro Stunde abgeschätzt werden. Bomben-Tritium ist an dieser Stelle im Grundwasser nicht nachweisbar. Das Reservoir-Volumen für das Grundwasser, welches am Versuchsort Migration in den Laborstollen fliesst, muss daher gross sein. Wahrscheinlich ist die Kluft in dieser Gegend mit einer grösseren Scherzone verbunden.

## Résumé

Dans une simple fissure du Laboratoire Souterrain du Grimsel, des essais de migration sont étudiés en matrice rocheuse granodioritique. Le but de ces essais est de valider les modèles de transport des radionuclides et de développer des techniques expérimentales. Ce rapport décrit le site choisi pour les essais de migration et présente l'instrumentation originale.

Les vitesses d'écoulement de l'eau qui entre dans le tunnel ont été estimées dans quatre différentes zones fissurées (lamprophyres et zones mylonitisées). D'après ces estimations, la location AU96m a été choisie parce qu'elle se présente favorablement pour les essais de migration. Cette fissure mylonitique était cependant presque inconnue en ce qui concerne la caractérisation hydrogéologique à l'échelle de 10 x 10 m. C'est pourquoi cette zone a été exploré à l'aide de forages. Dix forages ont prouvé que la fissure est un élément presque plan dans le massif saturé. Huit de ces forages produisent suffisamment d'eau pour mesurer la pression hydrostatique et pour échantillonner de l'eau. La plupart des forages sont équipés d'un système d'obturateurs triples qui isolent la fissure à l'entrée du forage. Des essais hydrauliques passifs ont prouvé qu'il existe une connection hydraulique entre les zones mylonitiques atteintes par les forages et que la transmissibilité de la fissure est d'environ  $0.6 \text{ m}^2/\text{j}$ . L'étude à long terme a montré une décroissance de la pression hydrostatique d'environ  $0.08 \text{ bar/a}$ , ce qui indique que le système hydraulique n'a pas encore atteint complètement un état stationnaire.

Des feuilles en matière plastique ont été fixées à la paroi du tunnel, à l'intersection avec la fissure. Ces feuilles permettent de mesurer le débit d'eau qui est environ  $0.5 \text{ l/min}$ , au site de migration. Lors de l'observation de phénomènes d'écoulement pendant les forages, et lors du remplacement de l'eau du site par une eau d'une composition différente pendant des essais injection – extraction, la vitesse d'écoulement a été estimée de l'ordre de quelques mètres par heure. La concentration en Tritium s'est montré d'être sous la limite de détection. Les auteurs concluent que le volume du réservoir d'eau, qui s'écoule vers le tunnel au site de migration doit être grand (plus de  $200 \text{ m}^3$ ). La fissure est probablement reliée à une importante zone de cisaillement.

# 1 Introduction

In the safety assessment of radioactive waste repositories the study of migration (i.e. transport behaviour of substances dissolved or suspended in groundwater) is of great importance. Such studies are a necessary prerequisite for adequately describing the performance of the geological barrier. Besides the physical transport mechanisms (advection, dispersion, matrix diffusion and others), the various chemical reaction processes along the flow path are of interest. Many of these chemical processes lead to a retardation of substances with respect to the flowing groundwater. Laboratory experiments provide essential data on the chemical aspects of transport. However, field migration experiments at well-described sites complement laboratory experiments in testing transport models (INTRAVAL, 1987) at a scale larger than that of laboratory systems. They help the accumulation up of know-how for investigations at future disposal sites (e.g. HADERMANN et al., 1988) and contribute to the improvement of instrumentation for the measurement of transport parameters. For these reasons, field migration experiments at NAGRA's Grimsel Test Site (GTS) were initiated.

The GTS in the central Swiss Alps is an underground facility in granitic rock about 400 m below the surface and has been operated since 1984 (NAGRA, 1985). In this drilled tunnel, a water bearing fracture has been selected for migration experiments where the transport behaviour of non-sorbing and sorbing tracers dissolved in the groundwater is studied. The interaction of sorbing tracers with the infill material of a water-saturated fracture is emphasized. It is acknowledged that data from field investigations alone have little chance for an unambiguous interpretation. Therefore, the experiment is complemented by a comprehensive laboratory program which includes characterisation of rock and groundwater, studies of nuclide/rock interaction (BRADBURY, 1989), and small-scale infiltration experiments with core material from the field site (BISCHOFF et al., 1987). Other underground sites in granitic rock, in which migration experiments are under way, are former mines at Stripa, Sweden (e.g. NERETNIEKS et al., 1982; ABELIN, 1986) and Fanay-Augères, France (e.g. LASSAGNE, 1983), and Canada's Underground Research Laboratory near the Whiteshell Nuclear Research Establishment, Pinawa, Manitoba (e.g. DAVISON and GUVANASEN, 1985).

The experiments at Stripa have provided useful information for the GTS migration experiments. The transfer of know-how from Sweden to Switzerland mainly includes the instrumentation of the site (see Section 3) and the methodology for the proposed migration experiments. Interpretational difficulties at Stripa made it apparent that a

good knowledge of the flow field in the fracture (see Section 5 and Appendix B) and of the groundwater chemistry (see BRADBURY, 1989) is very important. Water/rock interactions are emphasized more in the GTS migration experiments than in the Stripa tests.

This report summarizes preliminary model assessments used for site evaluation, describes the exploration and instrumentation of the site and gives the results of the flow-field characterisation. The mineralogical and geochemical characterisation of the fracture material and the description of the groundwater composition at the site are given in BRADBURY (1989). Appendix A presents additional data on the groundwater composition. Hydraulic modelling is discussed by HERZOG (1989).

## 2 Site Selection

At an early stage of the study, several locations in the GTS were examined for potential suitability for migration investigations. Four locations (A – D in Figure 1) were chosen as candidate sites and the following criteria were used to select the final location (HADERMANN and HERZOG, 1985a):

1. A fair amount of groundwater must discharge into the tunnel;
2. the geometrical structure of the water-carrying zone must be simple;
3. the groundwater composition must not be disturbed by man's activities;
4. the experiment should not be impaired by other activities at the GTS.

It was thought that calculated estimates of travel time, which were based on knowledge available at that time, would help in selecting the best of these four locations. However, the locations could not be differentiated with respect to hydraulic characteristics without further exploration and testing (HADERMANN and HERZOG, 1985b). The calculations showed that a non-retarded tracer would need hours to several weeks to be transported a distance of a few meters under the estimated flow conditions.

Location A, at LA309m (GTS metering; NAGRA NTB 85-34), initially considered the most suitable, is characterized by a simple fracture geometry and a distinct groundwater discharge to the tunnel. A reconnaissance borehole (SB 80.003) transects this fracture and a hydraulic connection between the packed-off fracture zone of the borehole and the tunnel was proven. When the tunnel drilling machine passed the fracture (July, 1983), the hydraulic pressure in the packed-off zone of the borehole dropped significantly (KEUSEN, 1989). The location is also near the administrative and technical facilities of the GTS and suffers extensive traffic. This would make experimental work difficult.

Locations B through D are near the south end of the GTS where it consists of two tunnels, a western and an eastern arm. A low rate of discharge to the tunnel is difficult to measure and made Location B (at AU72m, GTS metering) unattractive. A hydraulic connection with the reconnaissance boreholes SB 80.004 and SB 80.005 was not proven for Locations B and D, respectively. Location D (at AU160m) suffered additional drawbacks in that 1) the water chemistry is probably altered due to the extensive use of gunite in

**FLG** FELSLABOR GRIMSEL  
**GTS** GRIMSEL TEST SITE

- Situation
- 0 100m
-  Zugangsstollen/Access tunnel
  -  Fräsvortrieb/by tunnel boring machine
  -  Sprengvortrieb/excavated by blasting
  -  Zentraler Aaregranit ZAGR  
Central Aaregranite CAGR
  -  Biotitreicher ZAGR  
CAGR with high content of biotite
  -  Grimsel-Granodiorit  
Grimsel-Granodiorite
  -  Scherzone/Shear zone
  -  Lamprophyrl/Lamprophyre
  -  Wasserzutritt/Water inflow
  -  Sondierbohrung/Exploratory borehole
  -  US Bohrung/US borehole
  -  ZB Zentraler Bereich/Central facilities
  -  AU Auflockerung/Excavation effects
  -  BK Bohrlochkranz/Fracture system flow
  -  EM El.magn. HF-Messungen/-measurements
  -  FRI Klufitzone/Fracture zone investigation
  -  GS Gebirgsspannungen/Rock stresses
  -  HPA Hydr. Parameter/Hydr. parameters
  -  MI Migration/Migration
  -  MOD Hydrodyn. Modellierung/H. modeling
  -  NM Neigungsmesser/Tiltmeters
  -  UR Untertageradar/Underground radar
  -  US Seismik/Underground seismic testing
  -  VE Ventilationstest/Ventilation test
  -  WT Wärmeversuch/Heat test

A — A Schnitt/Section

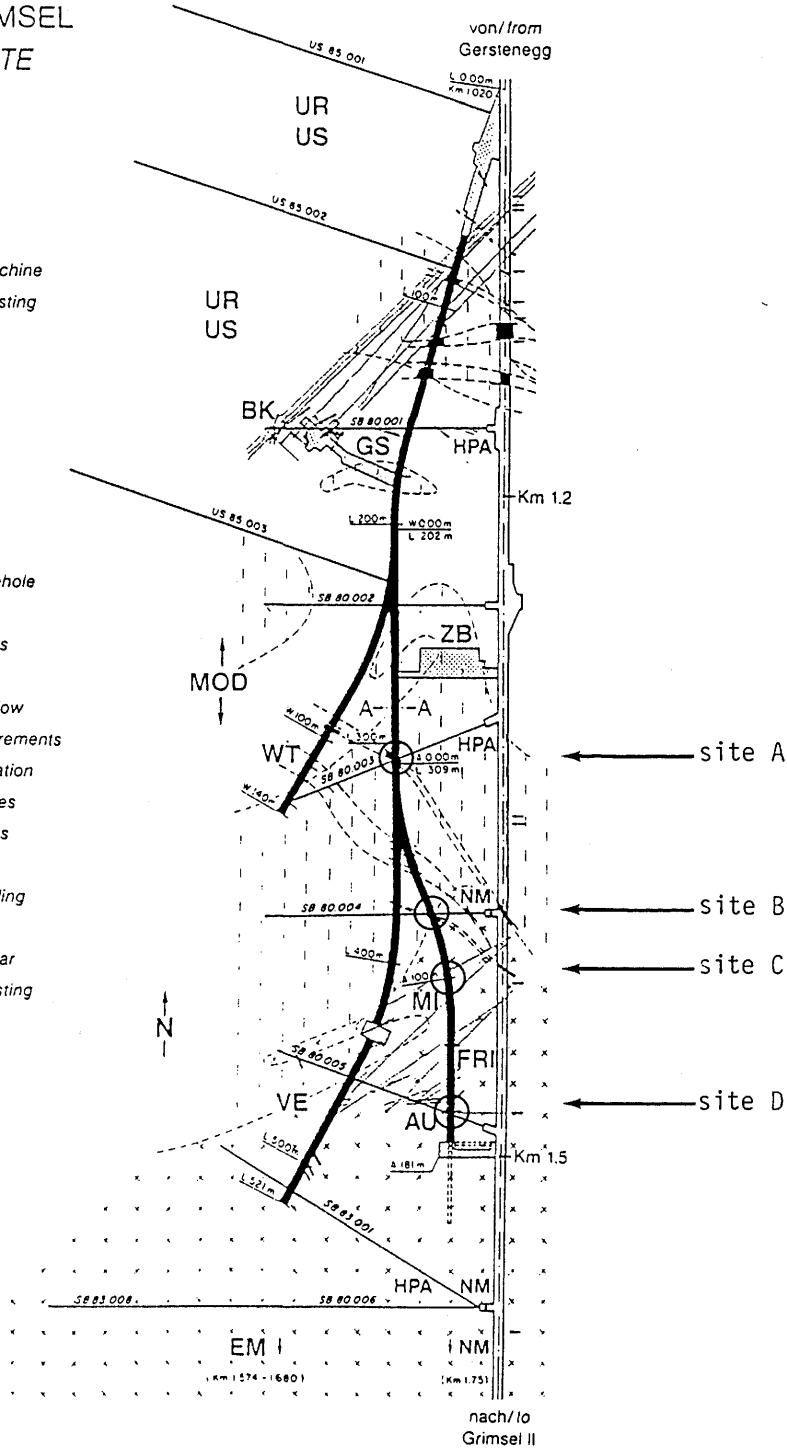
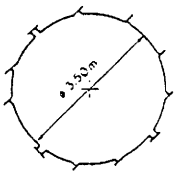


Figure 1: Map view of Grimsel Test Site showing most important geological features and locations of other investigations; arrows point to the four studied locations for migration investigations, A – D (from HADERMANN and HERZOG, 1985a).

the tunnel at this location, and 2) nearby boreholes and tunnels from a different experiment might affect the local flow field and cause unsaturated conditions. Thus the three locations, A, B, and D, were rejected.

At Location C in the eastern arm of GTS (see Figure 2; GTS metering: AU96m) an isolated shear zone with a narrowly-spaced set of a few fractures had been identified in otherwise unfractured rock. Here a migration experiment would not suffer significant interference with other experiments. Among these fractures, only one is water bearing. From measurements in the tunnel and, at a later stage, from inspection of a video recording of the borehole television log, the fracture aperture was estimated to be about one mm. The fractures are known to extend at least 70 m from the eastern tunnel arm and reach the main access tunnel and the western arm of the GTS. Easy access to a distinct outlet from the water-bearing fracture to the tunnel made location C attractive. During 1984, the outlet discharged about 0.2 L/min (KEUSEN, 1989). Although it was agreed that extensive drilling was needed to explore this location, location C was selected for the migration experiment. This site met with the criteria 1. – 4. established above. It was further concluded that the boreholes must be drilled such that the experiment could be performed on the small scale of a few meters at maximum (an area of about 100 m<sup>2</sup> in the fracture plane).

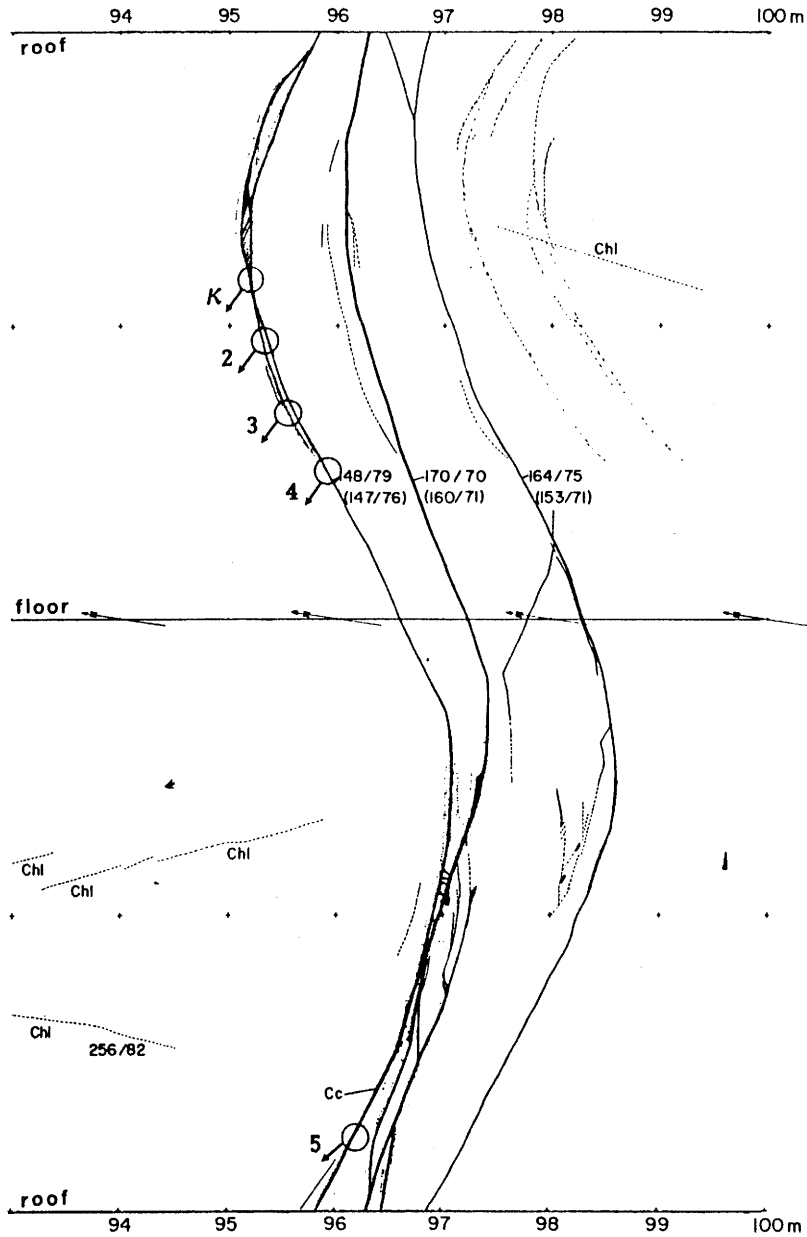


Figure 2: Planar projection of the shear zone at location AU96m (GTS metering) showing the water-bearing fracture system; Circles with arrows indicate channel outlets of groundwater; numbers near fractures indicate azimuth of dip, and dip, respectively; Chl = chlorite, Cc = calcite (modified from KEUSEN, 1989).

### **3 Site Instrumentation and Exploration with Boreholes**

After the decision that location C was the most promising for migration experiments, the next step was to obtain additional information about the fracture flow system. Instrumentation was provided to monitor the flow from the fracture to the tunnel. Boreholes were then drilled to provide access for hydraulic and tracer testing.

#### **3.1 Instrumentation at the Tunnel Wall**

The intersection of the tunnel with the water bearing fracture at location AU96m was instrumented for discharge measurements and sampling. Besides the main channel, five minor channels were identified with groundwater flow in the fracture. Polyethylene plastic sheets were attached to the tunnel wall at the fracture intersection, with methods developed for the Stripa study (modified after ABELIN, 1986). The size of the sheets was chosen such as to minimize losses of groundwater to the tunnel and each sheet separates one of the identified flow channels. Polypropylene tubing at the bottom of each sheet carries the collected discharge water to a flow meter. An additional large sheet covers most of the fracture including the individual sheets.

The outlet of the major water-bearing channel extends about 0.05 m along the fracture. An area of about 0.04 m<sup>2</sup> around this channel was planified and smoothed. A groove was then drilled to mount a circular teflon cap. To avoid water passing the cap, grooves were drilled in the rock into which the cap was fitted tightly with teflon O-rings. The dead volume in the inside of the cap is estimated to be about 0.02 L. On the top and the bottom of the cap, PVDF tubings allow sampling of water and draining the cap, respectively.

#### **3.2 Exploration With Boreholes**

A total of eight boreholes were drilled during 1986 and 1987 to explore the migration fracture and to provide access for hydraulic and tracer tests. All boreholes (except BOMI 87.011) were drilled downwards to avoid problems with the intrusion of air (especially O<sub>2</sub> and CO<sub>2</sub>). The first two exploration boreholes were drilled such that they intersected the fracture at a distance of about 10 m from the tunnel, one on the west (BOMI 86.004) and one on the east (BOMI 86.005) side of the tunnel (see Table 1

and Figure 3). Both boreholes built up a hydraulic pressure of about 1.5 bar with a measurable discharge of groundwater (see Table 1). Since the discharge of borehole BOMI 86.005 was smaller than that of borehole BOMI 86.004 by a factor of about 70, it was decided to drill additional boreholes inclined downward on the west side of the tunnel only (3rd quadrant of Figure 3b).

Table 1: Geological and technical information on the boreholes

Bore-hole no.	azimuth (°)	dip (°)	length (m)	depth of fracture (m)	packed-off zone (m)	hydrostatic pressure in fracture, Nov.27,1987 (bar)
BOMI 86.004	187.7	-15	24.1	20.7	19.6-21.3	1.48
BOMI 86.005	142.4	-18	16.0	15.7-15.8		1.47
BOMI 87.006	337.7	-36	12.4	8.1-8.5	8.0-8.7	1.44
BOMI 87.007	334.3	-19	13.9	10.7	10.0 – 13.9	–
BOMI 87.008	1.4	-56	5.8	2.1-2.3/3.2-3.3	2.0-3.6	0.53/0.55
BOMI 87.009	333.5	-39	12.8	9.4-9.7	9.2-9.9	1.45
BOMI 87.010	11.5	-19	8.5	6.6	6.2-6.9	0.55
BOMI 87.011	301.0	+13	22.0	18.3	17.6 – 22.0	–

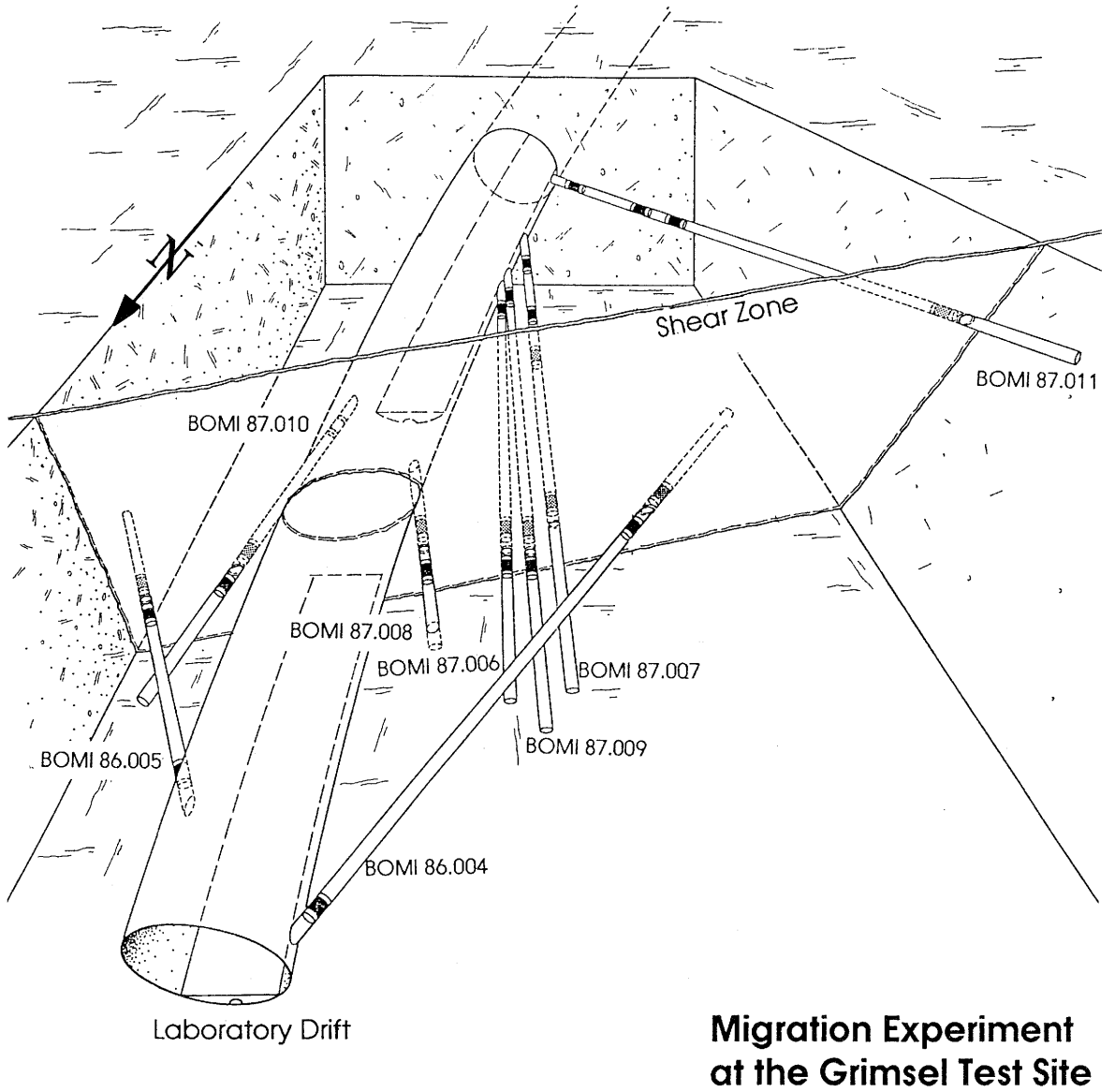


Figure 3a: Migration experiment location AU96m: 3-Dimensional view from north

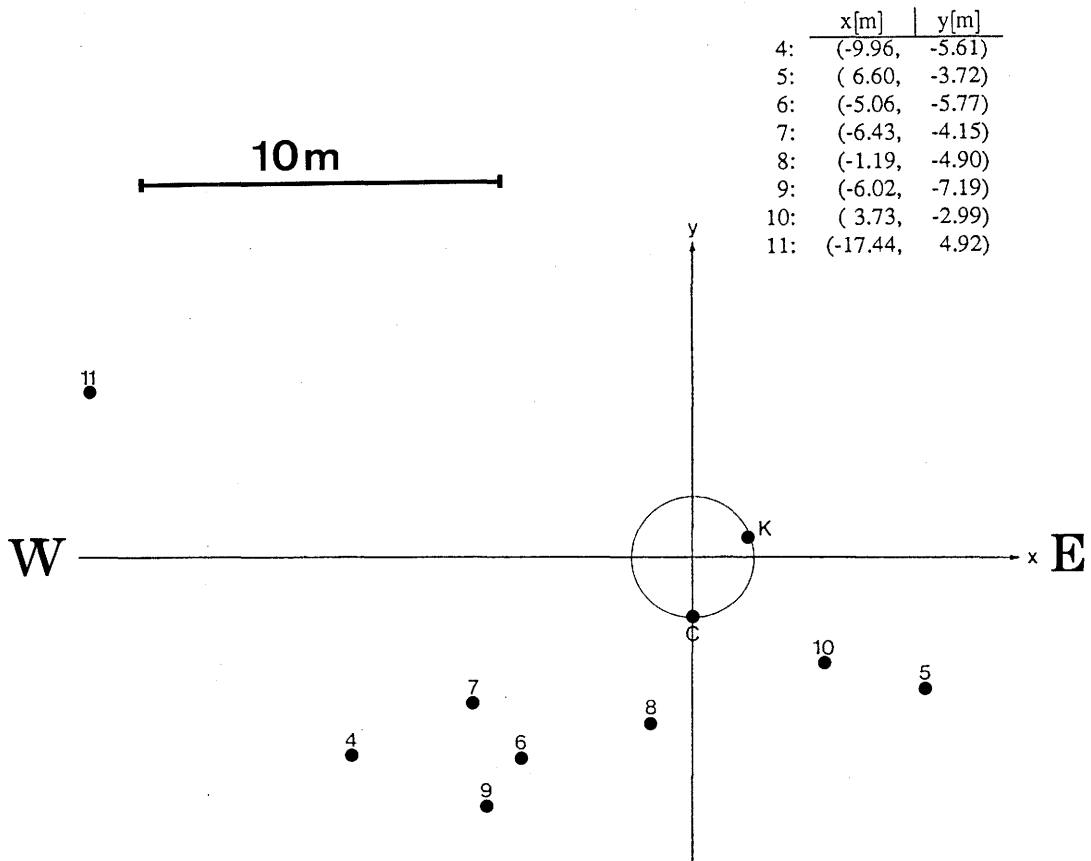


Figure 3b: Migration experiment location AU96m: Cross section through fracture plane, with points of intersection with boreholes; numbers indicate boreholes (from HERZOG, 1989).

In this second step, the boreholes BOMI 87.006 and BOMI 87.007 were drilled to intersect the fracture plane at an equal distance from the tunnel of about five meters. Borehole 87.007 is located between the tunnel and borehole 86.004, to explore the nature of the radial flow field converging on the tunnel. While borehole 87.006 was found to behave similarly to borehole 86.004, borehole 87.007 was found to be almost dry. A minor hydraulic pressure in this borehole of about 0.2 bar was built up only after about one year. An additional borehole, BOMI 87.008, was, therefore, drilled between the tunnel and borehole 87.006, to explore a possible flow path between 86.004 and the tunnel.

The purpose of the next borehole, BOMI 87.009, located at a distance of about five meters from borehole 86.004 and at about 2.5 m from borehole 87.006, was to provide an array of boreholes for injection–withdrawal tracer experiments. Additional exploratory boreholes, BOMI 87.010 located at the east side of the tunnel, and 87.011, located at the west side of the tunnel, were also drilled. Borehole 87.010 was drilled in an attempt to intersect the fracture channel which leads to the outlet of the main channel ("K" in Figure 3b). Borehole 87.011, which is inclined upward, is almost dry. With borehole 87.011, the extent of the fracture and the far field were explored. According to the flow model of HERZOG (1989), the flow field is asymmetrically radial, with a component pointing from the first quadrant of Figure 3b (upper left) on the tunnel. Borehole 87.011 was drilled accordingly. Overall, this exploration drilling program proved clearly the suitability of the chosen location for field migration experiments of the scale of a few meters. Hydraulic testing showed that the west side of the tunnel (3rd quadrant of Figure 3b) is more suitable than the other areas around the tunnel at this location (see below).

Drilling of each borehole could potentially have an adverse impact on the chemistry and flow–field properties of the fracture. During the drilling operations, the discharge to the tunnel, pH, oxygen, electric conductivity and temperature of the discharging water, and the hydraulic pressure in existing boreholes were monitored. Samples were taken occasionally for groundwater analyses. All of the flow producing boreholes responded to the drilling of additional holes with a pressure drop, just as the new borehole intersected the fracture. During the drilling of borehole 87.008, which is located closest to the tunnel (about 3 m, see Figure 3b), a breakthrough of oxygen and suspended solids was observed in the groundwater discharging to the tunnel at the outlet "K" of Figure 4. The maximum oxygen concentration occurred at Location "K" about 2.8 hours after the driller intersected the fracture. This breakthrough is interpreted as the travel time of

the oxygen-containing mixture of drilling fluid and groundwater from borehole BOMI 87.008 to the monitored outlet and corresponds to an estimate of groundwater flow velocity of 2 – 3 m/h. Oxygenated water injected during drilling of borehole BOMI 87.008 is expected to be flushed out to the tunnel because the hydraulic pressure in this borehole was lowest in comparison with that in the other boreholes.



### 3.3 Borehole Instrumentation

Systems with three water-inflated packers were installed in most of the boreholes to isolate the fracture interval and adjacent intervals on each side (Figure 5). A two-packer system was installed in the short borehole 87.008. Single mechanical packers were initially installed in the "nearly dry" boreholes 87.007 and 87.011. These were later replaced by inflatable systems capable of isolating an additional interval near the tunnel wall to investigate observed negative pressures.

Each packer is inflated and deflated through a separate polyamide-11 plastic line. Pressure in each packer is controlled individually and packer pressure is measured by a pressure gauge during hydraulic tests. Each packer-isolated interval has two lines connecting with equipment in the tunnel, one for flow and the other for measurement of interval pressure. The flow line opening is placed at the lowest possible point in the interval, and the pressure measurement line at the highest possible point. Only corrosion-resistant materials are used in the fracture interval. Some of the isolated fracture intervals are equipped with thermocouples.

For the tracer tests, an optical fiber has been included in two of the packer systems. These run from the fracture interval to the surface and allow in-situ measurement of fluorescent tracers. Tests can be performed under constant-drawdown or constant-discharge conditions. A data-acquisition system collects and stores the various measurements. Details on the instrumentation of the boreholes and the acquisition of data are given in THORNE (1990).

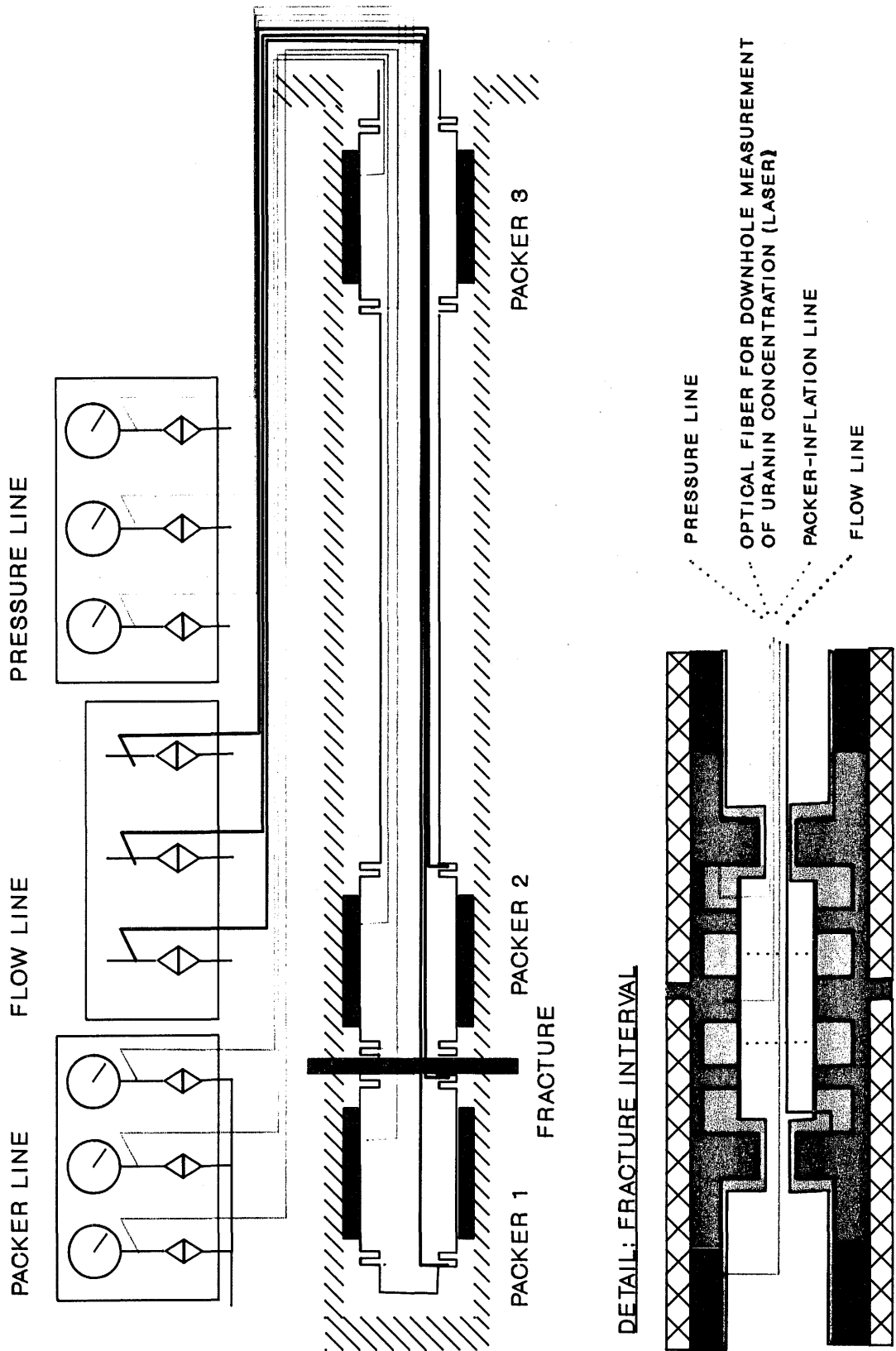


Figure 5: Schematic representation of standard triple packer arrangement in boreholes BOMI 86.004, 86.005, 87.006, 87.009, and 87.010 (from THORNE, 1990).

## 4 Flow Field

The flow field at location AU96m has been characterized by three observations: 1. Monitoring discharge rates from the migration fracture to the tunnel; 2. Monitoring hydraulic pressures in the boreholes and 3. Hydraulic testing of the borehole intervals with the fracture (see chapter 5). The flow field of the site was modelled by HERZOG (1989).

### 4.1 Discharge From the Migration Fracture to the Tunnel

Discharge to the tunnel from the outlet "K" at AU96m was measured during the period from the end of November, 1983 ( $t_0$ ), immediately after drilling the tunnel, through the end of July, 1984 ( $t_1$ ; KEUSEN, 1989). In this period of about 8 months, the discharge declined at an approximately logarithmic rate, from 0.45 l/min to 0.21 l/min. Figure 6 shows the discharge plotted on a logarithmic scale versus time ( $t$ ): The fitted straight line has a slope of about  $0.002 \text{ d}^{-1}$ . The slope is called the recession segment,  $\alpha$ , and is calculated as follows (e.g. BOUSSINESQ, 1903):

$$\alpha = \frac{1}{(t_1 - t_0)} \ln \frac{Q_0}{Q_1} \quad (1)$$

$Q_0$  and  $Q_1$  are the discharge rates at times  $t_0$  and  $t_1$ , respectively.

The existence of a logarithmic recession segment permits an estimation of the volume of the groundwater reservoir at the end of this early measurement period (WEYER, 1972; HOEHN, 1986):

$$V_1 = \int_{t_1}^{\infty} Q(t) dt \quad (2a)$$

$$Q(t) = Q_0 \exp[-\alpha(t - t_0)] \quad (2b)$$

which yields:

$$V_1 = Q_1/\alpha \quad (2c)$$

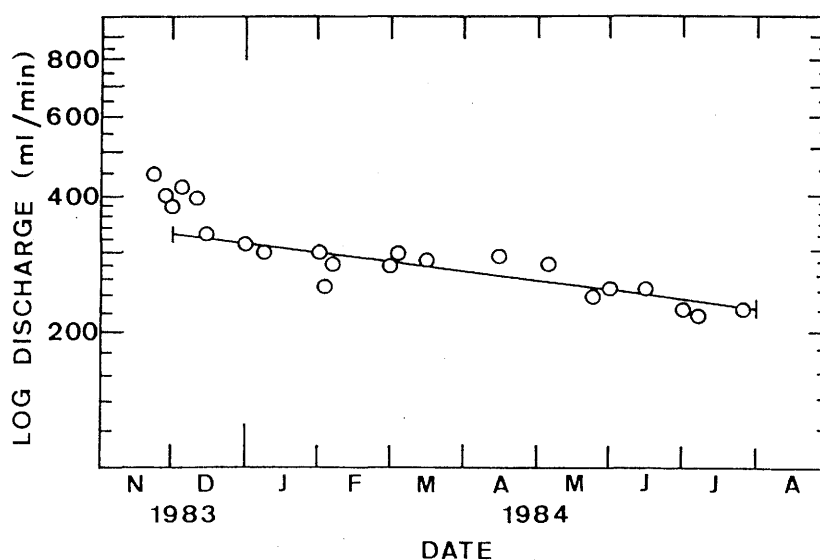


Figure 6: Time-series of groundwater discharge at outlet "K", and regression line showing exponential decrease ( $r^2 = 0.75$ ; errors  $\pm 20\%$ ).

The interpretation of the declining discharge at the outlet in the tunnel in 1984 suggested a high reservoir volume of about  $150 \text{ m}^3$ . The estimated fracture aperture of about one mm and the estimated extension of the fracture of about 100 m could not yield the necessary reservoir volume, especially when the observed channelling was considered. We rather believed that the waterbearing fracture is connected to one of the major shear zones of the GTS area which can be traced to the ground surface (KEUSEN, 1989). The absence of significant seasonal changes in the groundwater composition and temperature (BRADBURY, 1989), as well as very low tritium concentrations (see Appendix A), may further corroborate the assumption of a large reservoir in the aquifer.

A value of  $\alpha$  of about  $0.002 \text{ day}^{-1}$  indicates a small decrease of the discharge. Based on the ratio of reservoir volume over discharge rate, a travel time from the surface to the tunnel of at least one year is estimated.

From the results of early reconnaissance boreholes (NAGRA NTB 85-34), it was assumed that the fracture is water-saturated. A sump hole for the discharging groundwater of a depth of 0.3 m was drilled in 1986 (Borehole "C" in Figure 3b) which corroborates this assumption. This sump hole was drilled into the fracture at the bottom of the tunnel and discharges when open at about 0.6 l/min. It had to be packed-off because the outlet into the tunnel ran dry after about 20 minutes. Flow from the open sump borehole resulted in a transmissivity estimate of  $10^{-5}$  to  $10^{-6} \text{ m}^2/\text{sec}$ , with the methods described in Section 5.

The combined discharges of all outlets, which are sealed with sheets, amounted to about 0.5 l/min, in 1987. While the total discharge to the tunnel has not decreased significantly over the last two years, the relative contribution of the five different channels has changed, possibly due to borehole drilling and testing or to rock–mechanical displacements, as monitored by tilt meters. Pressure decreases in the boreholes due to drilling operations or hydraulic testing resulted in decreasing discharge rates to the tunnel (see Figure 7). As expected, the discharge rates of the different outlets into the tunnel decline logarithmically with time, during the period of withdrawal, and rise logarithmically with time, during the period of recovery. Changes in the contributions of the different outlets to the total discharge rate were also observed qualitatively. These changes are believed to result from micro–erosion and/or from channel clogging by particles and colloids carried by the moving groundwater. This effect may be caused by mechanical activities such as drilling or hydraulic testing in the fragile fracture–fill material (DEGUELDRE et al., 1989), or due to outgassing of the groundwater near the tunnel wall. This is corroborated by the observed breakthrough of suspended solids in the groundwater discharging to the tunnel during drilling of borehole BOMI 87.008. A breakthrough of oxygenated water was also observed and used to estimate the travel time of the groundwater in the fracture (see Figure 4). Groundwater flow in the vicinity of the tunnel is probably drastically enhanced as the tunnel acts as a drain.

## 4.2 Hydraulic Pressure in Boreholes

The hydraulic pressure in the packed–off interval of the boreholes which contains the fracture was measured under "natural" flow conditions. By "natural", it is meant that all boreholes are closed and a steady flow to the tunnel is established. It is clear that the distribution of hydraulic pressure would be different had the tunnel not been present (HERZOG, 1989). The boreholes can be separated into three groups based on similarities in response to hydraulic tests (see Section 5). Group 1 consists of boreholes 86.004, 86.005, 87.006, and 87.009 which exhibit stabilized pressures between 1.4 and 1.5 bar. Group 2 consists of boreholes 87.008 and 87.010, and borehole C, which exhibit pressures between 0.6 and 1.0 bar. Group 3 consists of boreholes 87.007 and 87.011 which produce almost no flow. The smaller pressures of group (2) with respect to the group (1) are believed to result from the proximity of group (2) to the tunnel, which acts as a drain. The almost complete lack of pressure in group (3) results from very low hydraulic conductivity at these boreholes and reflects the heterogeneity of the fracture. Hydraulic pressures in these two boreholes would be expected to increase

given an adequate amount of time with no disturbance in the flow system.

The hydraulic pressures were monitored intermittently in the isolated boreholes between November, 1986, and June, 1988, see Figure 8. Despite the influence of drilling between June and September, 1987, and some difficulties with the pressure transducers, a long-term trend of declining hydraulic pressure can be seen in this figure. The negative long-term pressure gradient was observed over 1986 – 1988 to be about 0.08 bar per year and is interpreted as a result of the influence of the tunnel.

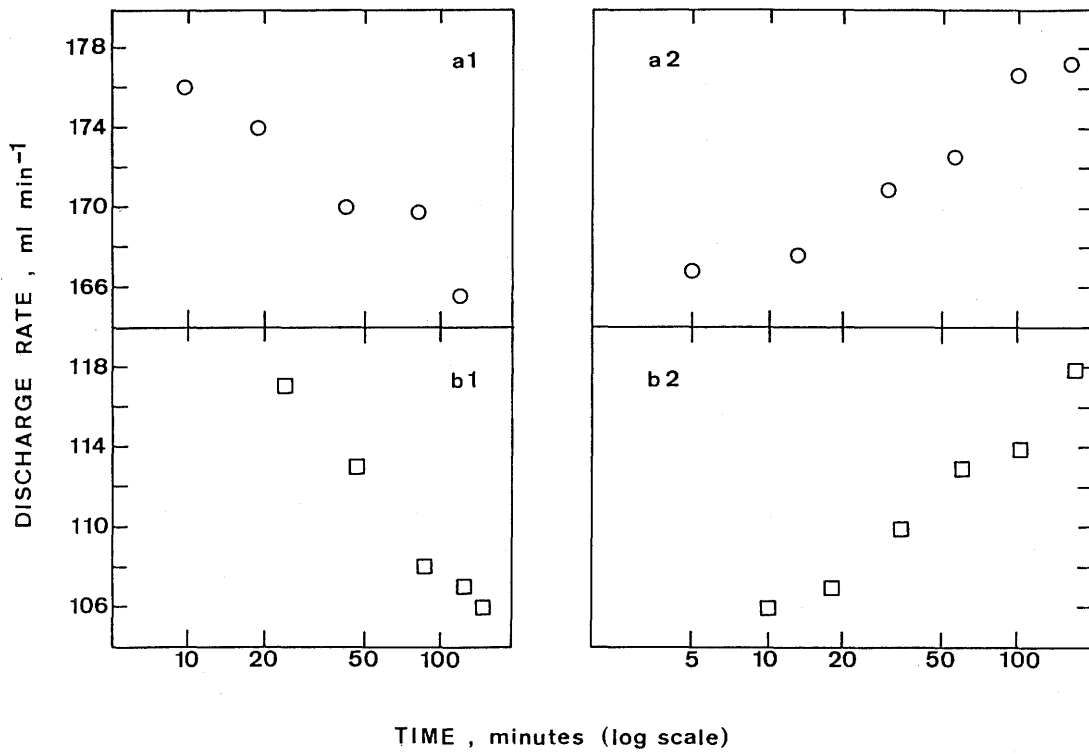


Figure 7: Discharge rates into sheets at tunnel wall of location AU96m as response to a constant-drawdown withdrawal test in borehole BOMI 86.004, December, 1986. a) Sheet 3, circles; b) Sheet 5, squares; 1) Withdrawal Period; 2) Recovery Period

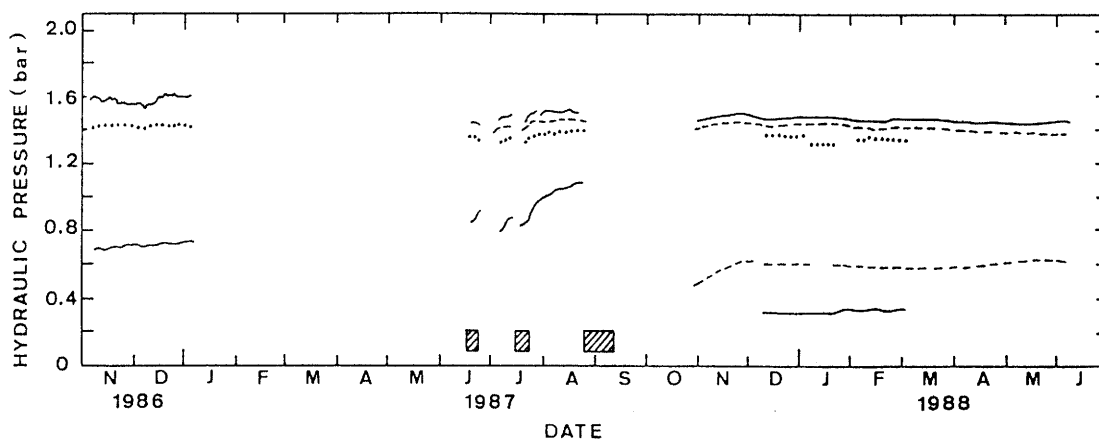


Figure 8: Time-series of the hydraulic pressure in the boreholes, dashed time intervals reflect drilling periods. Note long-term trend of decreasing pressure. Upper solid line, BOMI 86.004; upper dashed line, BOMI 87.006; dotted line, BOMI 86.005; lower dashed line, BOMI 87.010; lower solid line, C.

During the long-term, constant-flow hydraulic test, presented in Section 5.4, regular pressure changes on the order of about 0.01 bar, with a period of about 12 hours, were observed (Figure 9) which are interpreted as earth tide effects. In the late-time recovery phase (45 – 55 days) of this test, an additional pressure change of an even smaller magnitude was observed. This change was correlated to a drastic change in the barometric pressure of the atmosphere in this period. These pressure disturbances may have an effect on transport through the fracture by creating pressure differentials in the flow system.

Hydraulic pressures were also monitored in the isolated borehole intervals which did not include the fracture. In most boreholes, an interval between the fracture and the end of the borehole, and an interval between the fracture and the tunnel wall were isolated.

These intervals always showed lower pressures than the isolated fracture intervals.

Some intervals near the tunnel show negative pressures down to  $-0.6$  bars. This indicates that the granite matrix near the tunnel wall, but outside the water bearing fracture, is not saturated. Ventilating the tunnel results in a capillary force which dominates the flow regime and dries up the massive rock, on both sides of the fracture. The degree of undersaturation varies with time (see FRICK et al., 1988).

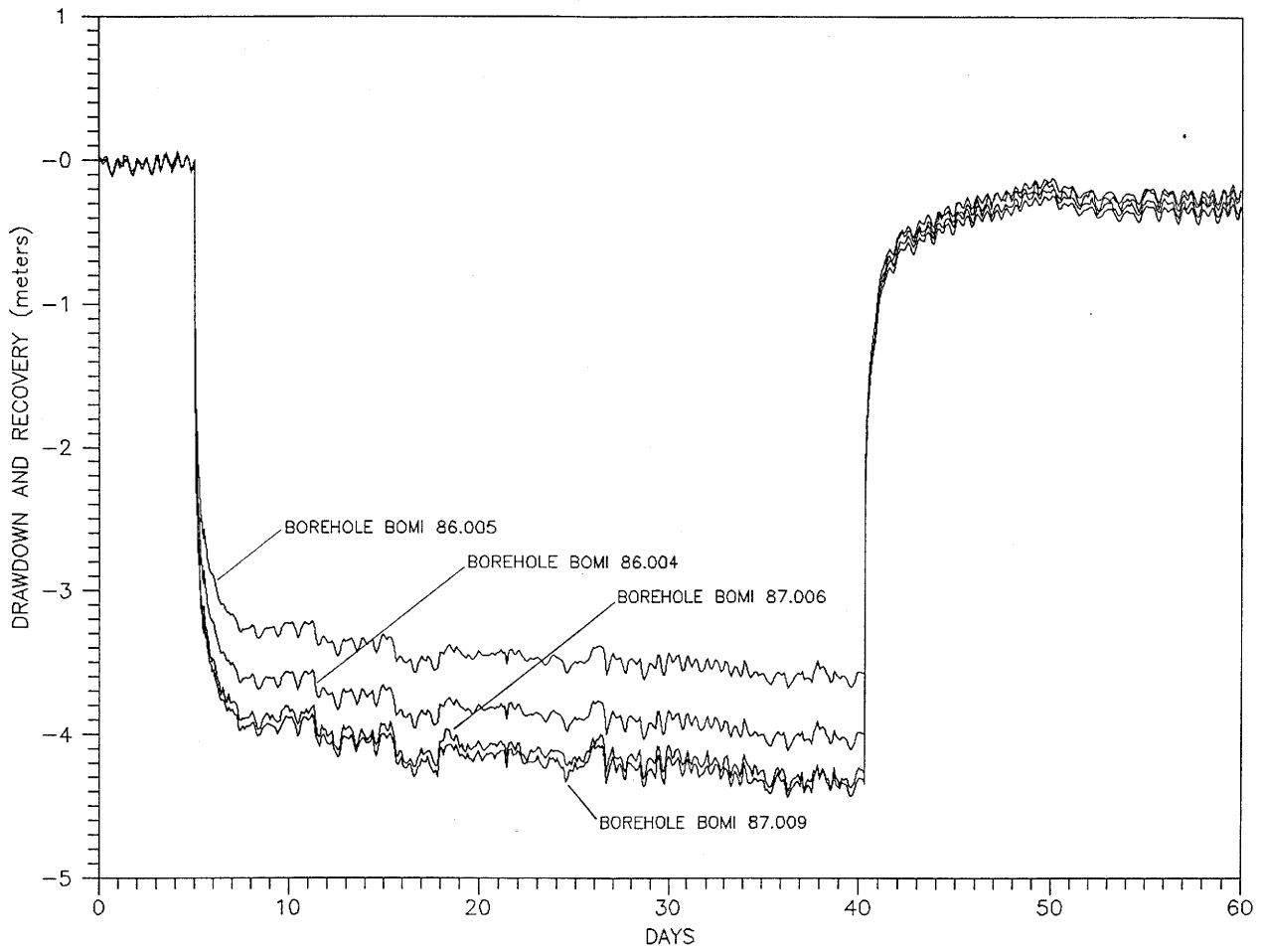


Figure 9: Pressure drawdown and recovery in selected boreholes as a response to a long-term, constant-discharge hydraulic test in borehole BOMI 87.009. From low to high drawdown: BOMI 86.005, BOMI 86.004, BOMI 87.006, and BOMI 87.009 (the tested borehole).

## 5 Hydraulic Tests in Boreholes

Several tests have been conducted in the exploration boreholes to evaluate hydraulic parameters of the migration fracture. The objective of these tests is 1) to provide input into flow models, and 2) to predict groundwater travel times. All the tests were "passive", i.e. no additional water was allowed to enter the flow system. Only the effects of drawdown and re-establishment of hydraulic potential (or pressure) in the boreholes and the effects of a constant discharge flow rate from the boreholes were analysed. The reason for this procedure is found in the overall aim of the Migration Experiment: the study of the chemical interaction of tracers dissolved in the groundwater with the rock surface of the fracture requires undisturbed geochemical conditions. The uncontrolled injection of additional water for hydraulic testing would have collided with this philosophy and was, therefore, abandoned from the beginning.

### 5.1 Preliminary Pulse Tests

The first hydraulic tests were conducted with the two then available boreholes, BOMI 86.004 and BOMI 86.005. Preliminary pulse tests (pressurized slug tests) were performed on the isolated fracture intervals of these boreholes during the period 25–26 September 1986. Their goal was to check, whether the fracture is transmissive away from the tunnel. These tests were conducted by opening the flow line from the borehole fracture interval for about 30 seconds to depressurize the interval, then closing the interval and monitoring the pressure recovery. Pressure responses were analyzed by the methods described by BREDEHOEFT and PAPADOPULOS (1980) and modified according to the suggestions of NEUZIL (1982). The resulting transmissivity values were about  $3 \cdot 10^{-6} \text{ m}^2/\text{sec}$  for borehole 86.004 and about  $5 \cdot 10^{-8} \text{ m}^2/\text{sec}$  for borehole 86.005. These values are regarded as qualitative estimates due to the limited area of influence of such tests and uncertain equipment compliance during the pressure build-up.

### 5.2 Methods for Hydraulic Test Analysis

The results of these early-tests showed that the fracture transmissivity was well within the range for the planned Migration Experiment. Therefore, the six new boreholes, described in Section 3, were drilled during 1987 to explore the fracture in more detail and

to provide facilities for injection, withdrawal, and monitoring of tracers. With all boreholes available, two types of hydraulic tests were conducted: a) single-borehole tests, and b) cross-hole interference tests. Single-hole tests use data from the tested borehole only, while cross-hole tests also use data from an additional observation borehole in which the hydraulic potential is monitored. For both types of tests several methods for the analysis were utilized. The equations for the calculation of transmissivity and the storage coefficient, and the references for these methods are given in Table 2.

Table 2: Methods for Hydraulic-Test Analysis

Method	Equation	Reference
Flow Period: Constant Drawdown	$T = \frac{2.3}{4\pi} \frac{1}{s_w \beta'}$	JACOB and LOHMAN (1952)
Flow Period: Constant Discharge	$T = \frac{2.3 Q}{4\pi \beta}$	COOPER and JACOB (1946)
	$S = 2.25 T (t_o/r^2)$	COOPER and JACOB (1946)
Steady State (Darcy's Law)	$T = \frac{2.3 Q}{\pi s_w} \log \frac{R}{r}$	e.g. LOHMAN (1972)
Recovery	$T = \frac{2.3 Q}{4\pi M}$	HORNER (1951)

T = Transmissivity

S = Storage coefficient

Q = Discharge rate

R = Radius of influence

r = Radius of borehole, for single-hole tests; distance to observation borehole, for cross-hole tests

$s_w$  = Drawdown in tested borehole during flow period

M = Slope of straight line fitted to  $s_w$  against  $\log(t_D)$ , where

$t_D$  = dimensionless time =  $(t_c + \Delta t)/\Delta t$

( $t_c$  = production time,  $\Delta t$  = shut-in time)

$\beta'$  = Slope of straight line fitted to  $(s_w/Q)$  against  $\log(t_c/r^2)$

$\beta$  = Slope of straight line fitted to  $s_w$  against  $\log(t_c)$

$t_o$  = Time where straight line intercepts the drawdown = 0 axis.

The equations for “constant drawdown”, “constant discharge” and “recovery” represent an approximate solution, the so called straight-line solution to the groundwater flow equations. The approximate solution is valid and the data expected to plot on a straight line, when time (t) and radial distance (r) are such that  $r^2 S/4Tt \leq 0.01$ . To calculate the storage coefficients, only the conditions of constant discharge during crosshole tests were used.

The equation for “steady-state” conditions uses the data at the end of the flow period. For the cross-hole steady state analysis, the final flow rate, the drawdown, the assumed radius of influence, and the radial distance between the tested and the observation borehole (see Table 3) were input to the radial flow equation. The radius of influence is a potential source of error because the value has to be assumed. However, the calculated transmissivity is proportional to the logarithm of R and is, therefore, not very sensitive to incorrect values.

Table 3: Calculated radial distance between test zone and observation zone

Tested borehole	Observation borehole	Radial distance between boreholes (m)
86.004	86.005	16.56
	87.006	4.81
	87.008	8.96
	87.009	4.16
	87.010	13.85
	C	10.57
87.006	87.008	4.16
	87.009	1.62
	87.010	9.13
	C	6.34
87.008	87.009	5.57
	87.010	4.89
	C	2.93
87.009	87.010	10.53
	C	7.99
87.010	C	3.83

A third method for the calculation of transmissivity, the HORNER (1951) "recovery" method, uses the recovery of the drawdown from both the tested and the observation borehole following hydraulic tests. This method, like the COOPER and JACOB method, assumes a constant-discharge flow period which introduces a potential error in the analysis.

### 5.3 Evaluation of Constant-Drawdown Tests

Constant-drawdown withdrawal tests were conducted with boreholes 86.004 and 86.005 during November and December 1986, respectively, before drilling the additional exploration boreholes. Each borehole was tested by opening the flow line from the isolated fracture interval and allowing water to flow out under atmospheric pressure conditions. The flow rate from the test interval was measured continuously and the fracture-interval pressures in the tested borehole were measured by a piezoresistive pressure transducer connected to the separate pressure measurement line. In addition, the pressure response in the isolated fracture interval of borehole BOMI 86.004 was measured during the test of borehole BOMI 86.005 so that cross-hole test analyses could be conducted. However, no conclusive response was seen at the borehole 86.004. The lengths of the flow periods were 140 min for borehole 86.004 and 225 min for borehole 86.005. The response of the discharge rate into the tunnel at location AU96 m to the testing of borehole BOMI 86.004 is seen in Figure 7.

Constant-drawdown withdrawal test similar to those described above were conducted in August 1987 with the new exploration boreholes. Information concerning each of the constant-drawdown tests conducted in November/December 1986 and August 1987 is provided in Table 4. In boreholes BOMI 87.007 and 87.011 the fracture was not permeable enough for hydraulic testing. The very low hydraulic conductivities encountered at these boreholes show the limits of the assumption of a homogeneous aquifer. Boreholes BOMI 86.004 and 86.005 were tested again because of the possibility of collecting data from additional observation boreholes with the cross-hole methods. An example of the hydraulic potential in the fracture intervals of the observation boreholes is shown graphically in Figure 10 for various times during the constant-drawdown test in borehole BOMI 87.006.

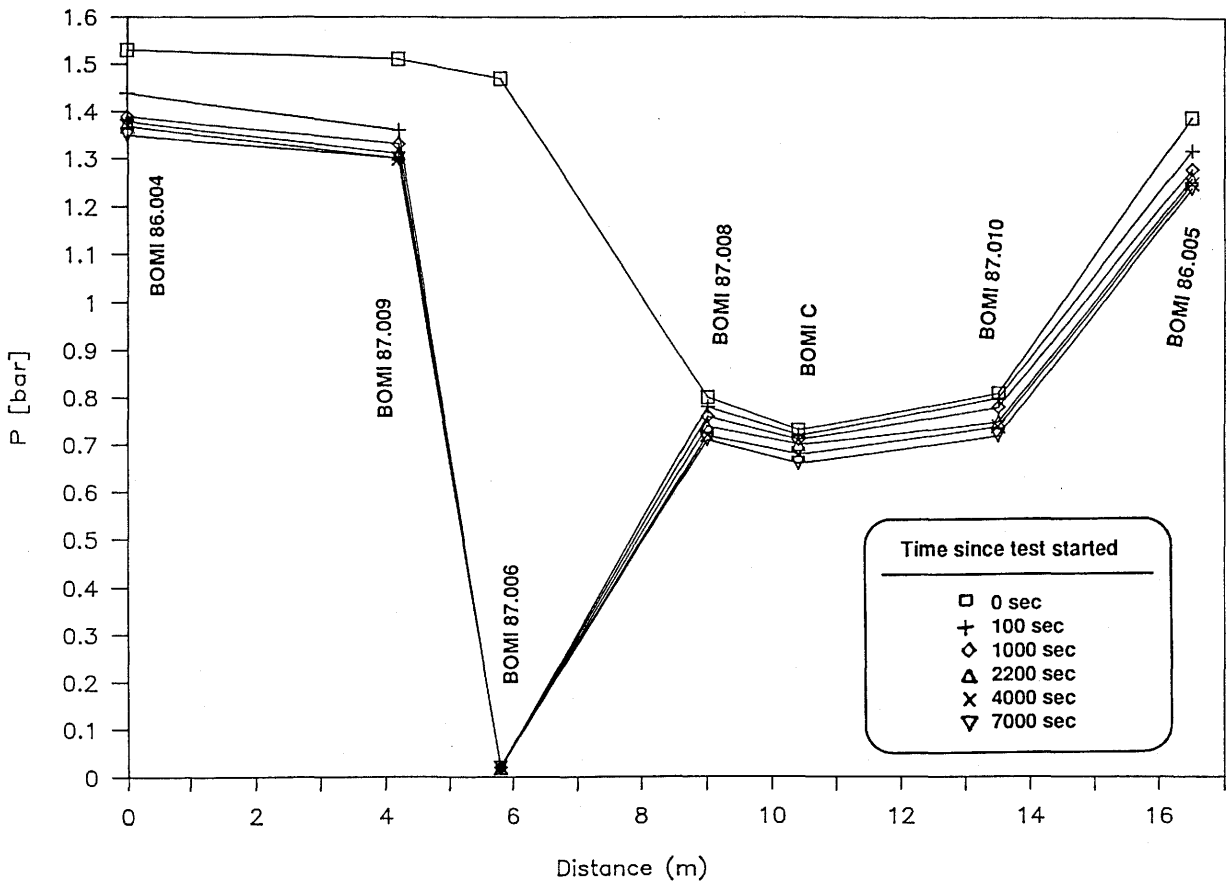


Figure 10: Distribution of hydraulic pressure in selected boreholes, along a transect from borehole BOMI 86.004 to BOMI 86.005, during a constant-drawdown test in the flowing borehole BOMI 87.006.

Table 4: Summary of constant-drawdown withdrawal tests

Tested Borehole	Test Date	Flow Period (min)	Recovery Period (min)	Discharge Range (ml/min)
86.004	06-11-86	140	923	625 – 522
86.004	08-12-87	169	978	840 – 630
86.005	16-12-86	225	136	18 – 13
86.005	10-12-87	304	16	168 – 12
86.006	26-08-87	116	987	660 – 360
86.008	28-08-87	278	4480	840 – 480
86.009	27-08-87	167	1208	2400 – 1380
86.010	31-08-87	82	738	1320 – 540

Transmissivity was calculated with the data from the flowing borehole by applying the method of JACOB and LOHMAN (1952) for the flow-period data. In this method, the reciprocal of the decreasing flow rate is plotted against log time. After a certain point in the test, this plot should theoretically follow a straight line whose slope is inversely proportional to the transmissivity. Hydraulic parameters calculated from the various methods for each constant-drawdown test are given in Appendix B, Table B1. The transmissivity values calculated from the JACOB and LOHMAN method are given under the heading "Flow Period" and in the top row for each tested borehole. An example of the plotted data and calculation of transmissivity is shown in Figure 11. The results are discussed in Section 5.5.

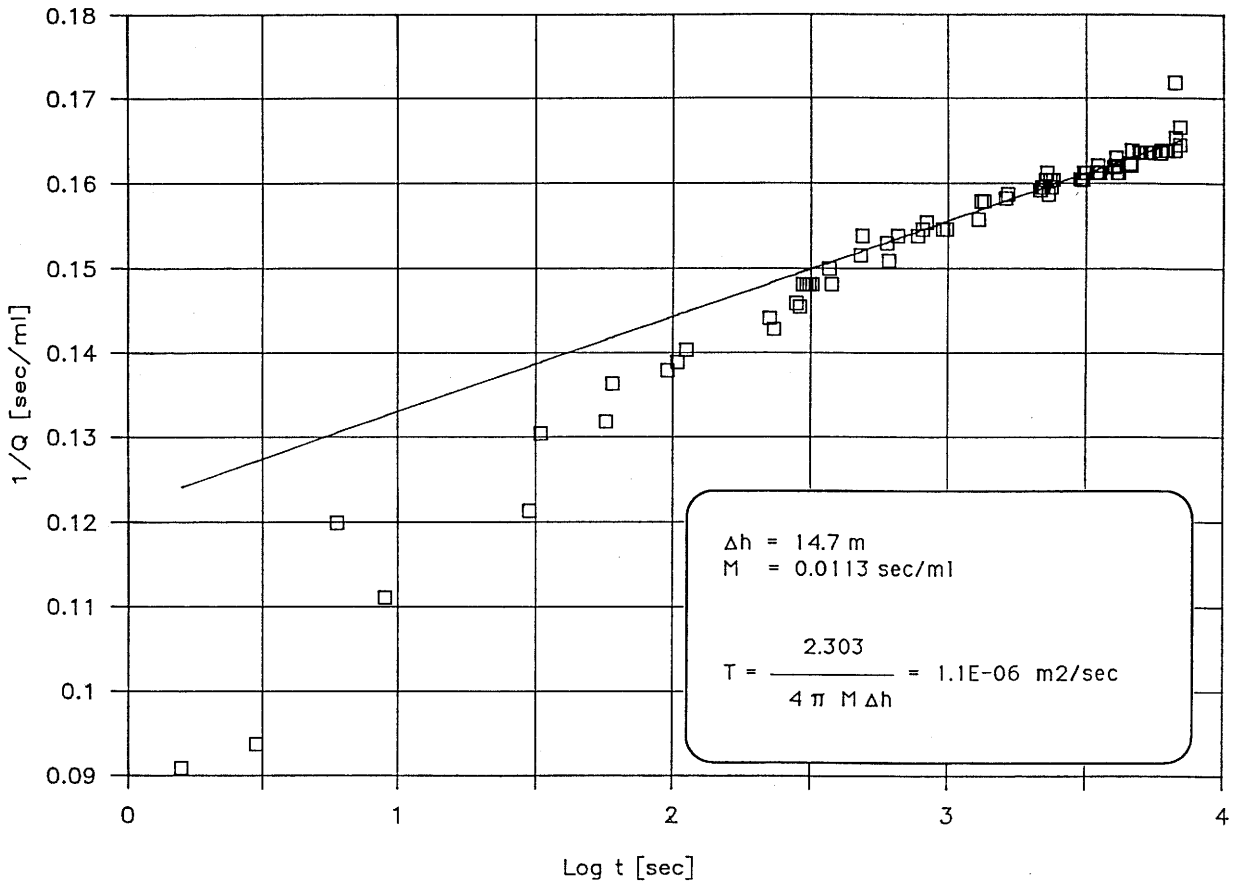


Figure 11: Analysis (after JACOB and LOHMAN, 1952) of flow-period data from a constant-drawdown test in the flowing borehole BOMI 87.006, with regression line (from THORNE, 1990)  $M\Delta h = \alpha$  in text.

The JACOB and LOHMAN method is not applicable to data from interfering observation boreholes because the response in these boreholes is a decreasing pressure due to the flow at the tested borehole. The data were, therefore, analysed with the method of COOPER and JACOB (1946) to determine transmissivity and storage coefficient. The decrease in pressure is plotted against the log of the flow time. This should give a straight-line plot at late time whose slope is inversely proportional to the transmissivity. This method is a simplification, since the solution is based on the assumption of constant discharge into the tested borehole. This introduces a potential error. However, at late time, the change in flow rate is small and the results of the COOPER and JACOB analysis will approach the correct value. The final discharge rate was used in the calculation where the constant-discharge value is required. The results of the COOPER and JACOB method for each of the interference tests are presented in Appendix B, Table B1, under the heading "Flow Period" and in the row for the particular observation borehole. An example of plotted data and a transmissivity calculation are given in Figure 12.

In Table B1, storage coefficients are also given which were calculated with the COOPER and JACOB method. In the plot of Figure 12, the straight-line interpolation of the data is extrapolated to the x-axis to obtain the value of  $t_0$ .

Transmissivity was additionally calculated from each of the observation boreholes as well as from the tested boreholes by assuming that steady-state flow conditions exist at the end of the flow period. The results are listed under the heading "Steady State" in Table B1 of Appendix B.

The method of HORNER (1951) was used for analysis of the pressure recovery data from both the tested and observation boreholes following the constant-drawdown withdrawal tests. This method, like the COOPER and JACOB method assumes a period of constant discharge which introduces a potential error in the analysis. The recovery pressures are plotted against the log of a dimensionless function of time. At late times, equivalent to small dimensionless times,  $t_D$ , the data should plot as a straight line with a slope inversely proportional to the transmissivity. The results of the transmissivity calculations from the HORNER method are given in Table B1 under the heading "Recovery". An example of plotted data and a transmissivity calculation are given in Figure 13.

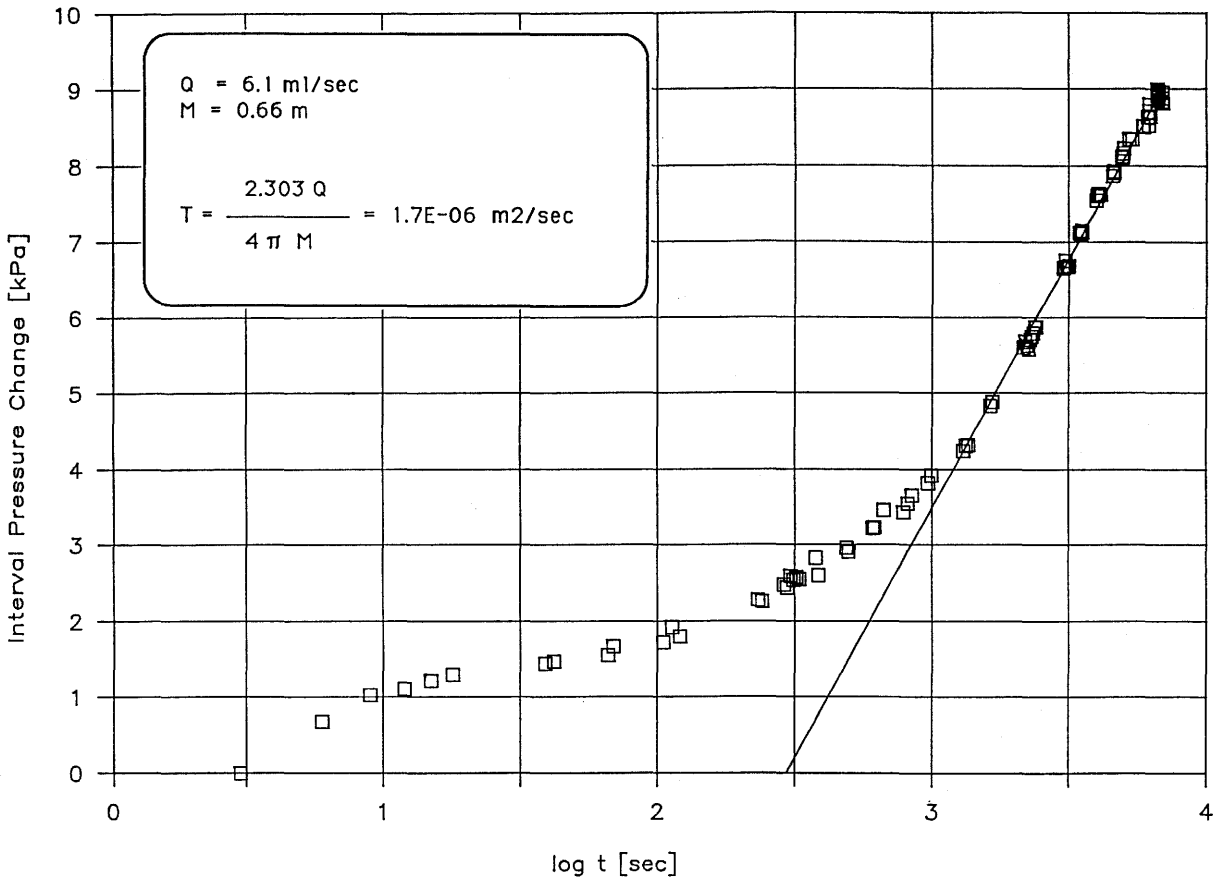


Figure 12: Analysis of pressure decline (after COOPER and JACOB, 1946) in borehole BOMI 87.008 as a result of a constant-drawdown test in the flowing borehole BOMI 87.006; with regression lines (from THORNE, 1990)  $M = \beta$  in Table 2.

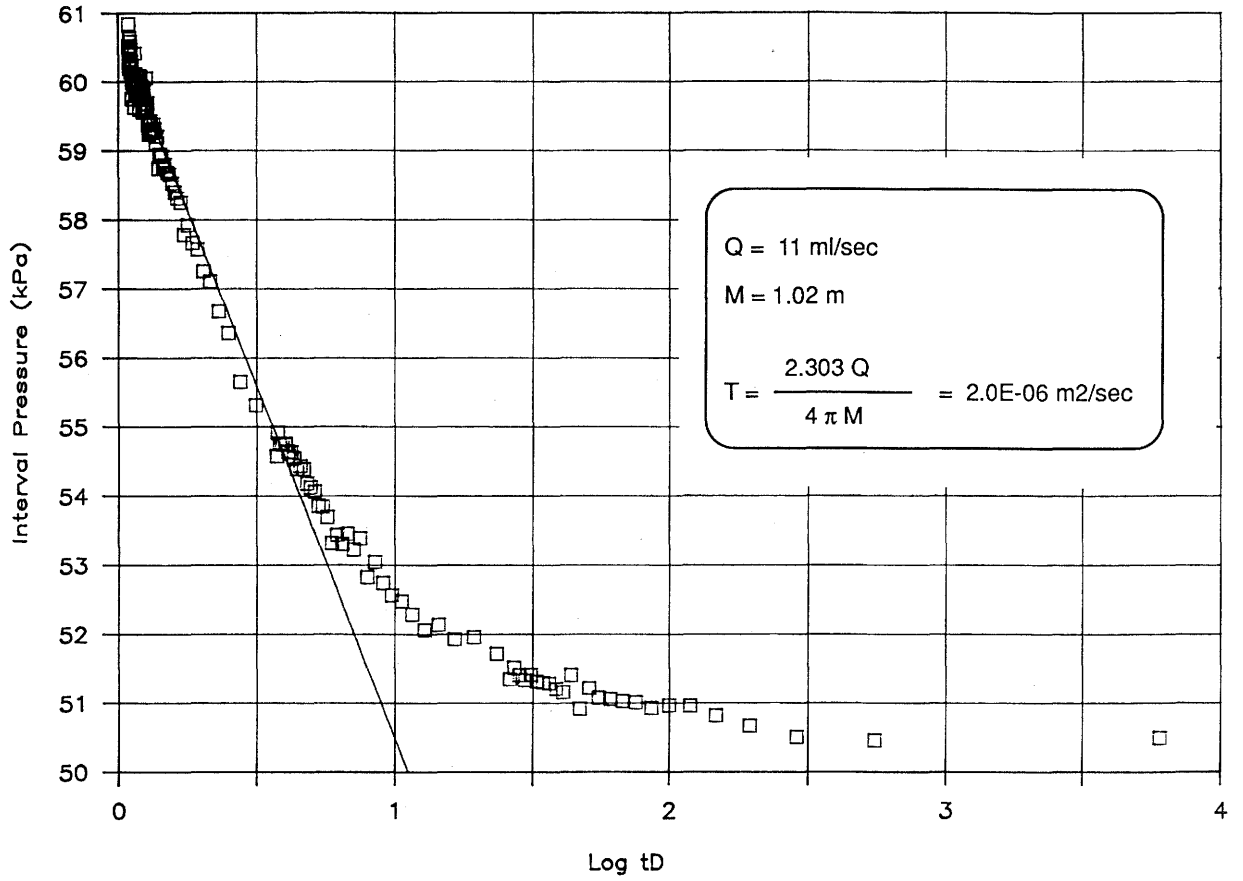


Figure 13: Analysis of pressure recovery (after HORNER, 1951) in borehole BOMI 87.010 as a result of the constant-discharge test in borehole BOMI 86.004; with regression line (from THORNE, 1990).

## 5.4 Evaluation of Constant-Discharge Tests

Because of the uncertainties in the use of the COOPER and JACOB, and HORNER methods of analysis for the constant-drawdown tests, constant-discharge tests were conducted on two of the boreholes. Constant-discharge tests are more difficult to perform, since the flow rate must be controlled and kept constant under changing interval pressure conditions. However, they have a great advantage over constant-drawdown tests because of the more reliable analysis of the observation borehole data. Constant-discharge tests have an additional advantage in testing higher permeability intervals, where the interval pressure does not immediately go to the atmospheric pressure when the flow line is opened. This can occur if the flow line is not large enough for the initial flow rate and can cause further uncertainty in the analysis as the test is conducted under neither constant-discharge nor constant-drawdown conditions.

Constant-discharge tests were conducted with boreholes 86.004 and 87.009 during 1987. Information on these tests is provided in Table 5. The values of transmissivity and storage coefficients determined from these tests are provided in Table B2 (Appendix B). The analytical methods for transmissivity were identical to those described above for the constant-drawdown tests, except that the flow period data from the tested borehole was analysed using the COOPER and JACOB method for constant-discharge tests, rather than the JACOB and LOHMAN method. For the storage coefficient, the straight-line interpolation of the data in Figure 12 is extrapolated to the x-axis to obtain the values of  $t_0$ .

Table 5: Summary of Constant-Discharge Withdrawal Tests

Tested Borehole	Test Date	Flow Period (min)	Recovery (min)	Discharge (ml/min)	Test Interval Pressure (bar)
86.004	09-12-87	325	1090	510	1.48 - 0.29
86.004	10-12-87	101	1007	720	1.48 - 0.01
87.009	01-09-87	195	—	1'170	1.48 - 0.53

## 5.5 Discussion of Constant–Drawdown and Constant–Discharge Tests

In this section the results of the hydraulic tests given in Tables B1 and B2 of Appendix B will be discussed. Firstly, mean transmissivity values of the different methods are compared; secondly, the cross–hole transmissivity values from one to the other chosen borehole are compared; and then, the values for the storage coefficient are briefly discussed.

Mean transmissivity values were calculated and given in Table 6 for the different methods. Where ranges are given in the transmissivity compilation of Tables B1 and B2, both extreme values were considered for the means. The “recovery” values of borehole BOMI 87.009 were all given as ranges and were, therefore, not considered in Table 6. This table shows that the boreholes BOMI 86.004, 87.006 and 87.009 are located in a relatively permeable domain and are hydraulically best suited for migration experiments among the exploration boreholes.

Table 6: Mean Transmissivity Values

Borehole BOMI 86.0/ 87.0, Nr.	Method	Number of values	Transmissivity, $10^{-6}\text{m}^2/\text{sec}$	
			arithmetic mean $\mu$	standard deviation, $\sigma$
04	Flow Period A	9	5.1	9.0
	" B	14	5.0	8.1
	Steady State A	8	15	32
	" B	14	14	31
	Recovery A	5	1.5	0.7
06	Flow Period A	7	1.8	0.4
	Steady State A	7	3.5	2.2
	Recovery A	7	1.8	0.4
08	Flow Period A	9	2.9	1.8
	Steady State A	7	5.1	3.8
	Recovery A	9	1.4	1.0
09	Flow Period A	7	2.9	1.0
	" B	7	2.4	0.7
	Steady State A	7	3.8	2.6
	" B	7	5.1	4.0
10	Flow Period A	7	2.0	1.0
	Steady State A	7	5.6	4.5
	Recovery A	7	2.2	1.8

A = constant drawdown; B = constant discharge

For the boreholes BOMI 86.004 and 87.009, the values of the constant-drawdown tests could be compared with those of the constant-discharge tests. They agree well within about 25 per cent. In general, the flow-period data of the constant-drawdown test revealed the smallest standard deviation relative to the mean of all methods of analysis, with values of  $\sigma/\mu$  below one. Therefore, this method seemed to be most reliable for further interpretations. The values varied systematically for the different methods: "steady-state" values were highest and "recovery" values were lowest. The transmissivity calculated from this method is expected to be greater than in reality, because steady-state conditions had probably not been reached at the end of the tests. At steady state, the discharge flow rate will be lower and the drawdown greater than the values used in the calculation. It is not known whether the "recovery" values are smaller than the others because of the assumption of a constant discharge period.

The flow-period, constant-drawdown and the recovery data of the single-hole tests in boreholes BOMI 86.004, 86.005, 87.006, 87.008 and 87.009 were exploited in a flow model of the area with a heterogeneous transmissivity field (HERZOG, 1989). His values differ slightly from those given in Table 6 because the latter included the results of the cross-hole tests. Geometric mean values of the cross-hole transmissivities are higher than those of the single-hole values by a factor of about 5, although it is not obvious why the values of the two test types differ systematically. The geometric mean was taken for this purpose because it was assumed that the spatial variability is log-normal (e.g. GELHAR and AXNESS, 1983).

Under the assumption upon which the tests are based, cross-hole tests should yield the same transmissivity results for both interfering boreholes. Any differences in the two values may give some insight into the heterogeneous flow geometry. Differences were calculated with the flow-period transmissivity data of the constant-drawdown method of Table B1 for the boreholes in which the fracture has been shown to be relatively permeable, i.e. boreholes BOMI 86.004, 87.006, 87.008 and 87.009. In the two-well tests in which borehole BOMI 86.004 is involved transmissivity varies by less than a factor of 1.3. In the two-well tests of borehole BOMI 87.006 with BOMI 87.008 and 87.009, however, transmissivity varies by more than or equal to a factor of two. It seems, therefore, that the fracture geometry is more homogeneous near borehole BOMI 86.004 than near 87.006.

In Tables B1 and B2 the storage coefficient varies by more than three orders of magnitude. These values have to be taken with caution as the extrapolations shown on the graph of Figure 12 were drawn on a log scale. This makes the storage coefficient more sensitive to the validity of the assumption of an "infinite aquifer extent" than transmissivity. Errors are easily introduced because this assumption is not valid, as is shown in the next section.

## **5.6 Long-Term, Constant-Discharge Test of Borehole BOMI 87.009**

During January and February 1989, a long-term constant-discharge withdrawal test was conducted in borehole 87.009 to better define the hydraulic system of the migration fracture. The objectives of the long-term test were to examine the possible existence of flow boundaries within the fracture system, examine the effect of long-term pumping on the drift outflow, and to analyze the pressure-recovery data using an analytical model

developed specifically for fractured rock.

The fracture interval of borehole 87.009 was pumped for 35 days at a rate of 340 ml/min ( $\pm 10$ ml/min). Drawdown and, following pumping, pressure recovery were monitored for an equal period of time (see Figure 8). Continuously monitored data included flow rate and interval pressure of the pumping borehole, pressure data for each of the observation boreholes penetrating the fracture and the outflow of water from the fracture to the drift.

During the long-term test a doubling of the slope of the drawdown and recovery data were recognized when plotted against the log of time. Figure 14 shows data from observation borehole BOMI 86.004. An analysis with image borehole theory (FERRIS et al., 1962) indicated the possible existence of impermeable boundaries in the water-bearing fracture. Early-time data from the drawdown observations in boreholes BOMI 86.004 and 87.006 indicated that after about 100 minutes, a boundary effect could be found whose position would be at a distance of 25 – 30 m from the tested borehole BOMI 87.009. An alternative explanation for this phenomenon relates to the geometric boundaries of the tunnels which also might affect the drawdown and the recovery.

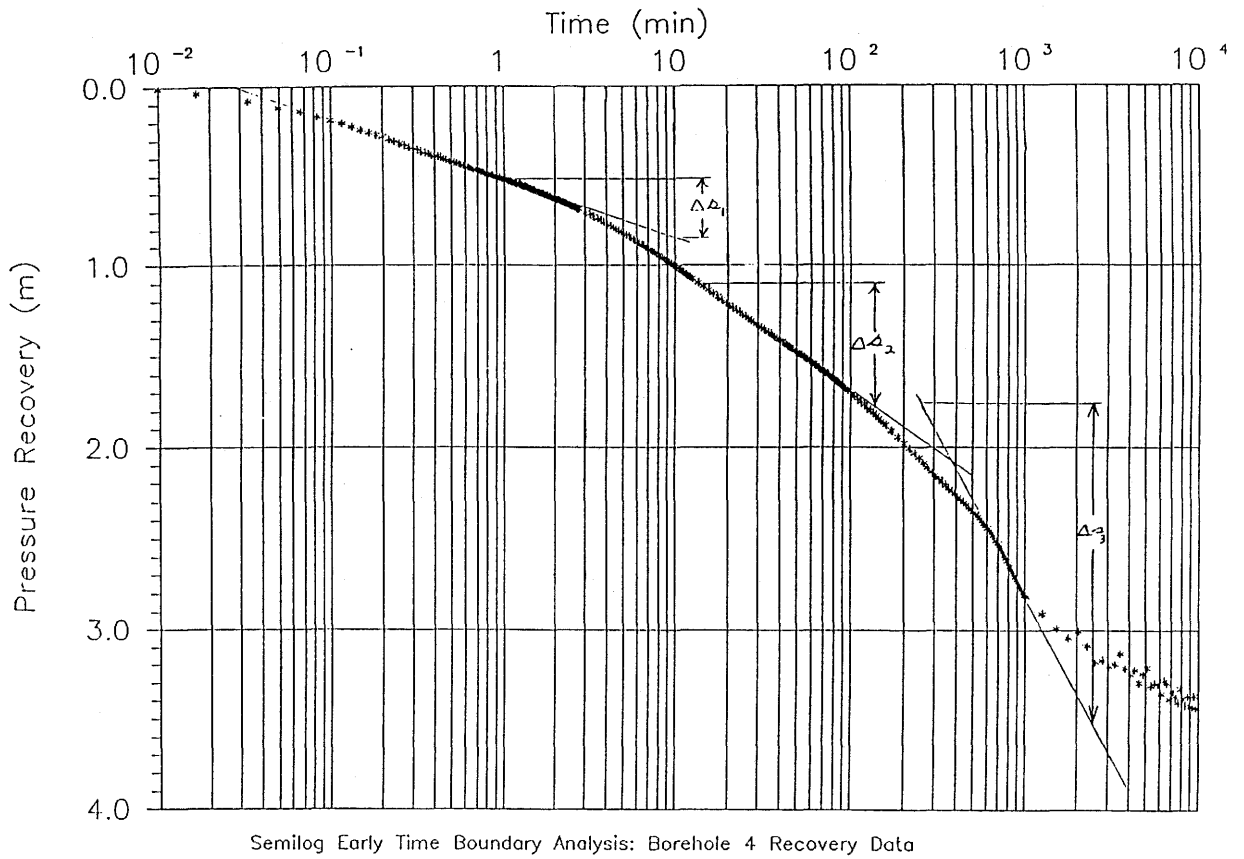


Figure 14: Pressure response of borehole BOMI 86.004 to long-term constant flow test in borehole BOMI 87.009. Note doubling of slope of drawdown ( $\Delta s$ ) plotted against log time (from GEMPERLE, 1990).

The drift outflow rate also reacted quickly to pumping and showed a steady decrease during the first 2000 minutes (about 33 hours) of pumping. After this time, nearly half of the pumped water from BOMI 87.009 was "captured" water from the drift outflow.

A double-porosity, fracture-flow analytical model was utilized to analyze the early-time recovery data from the long-term test. The analytical model utilized is discussed in detail by BOURDET and GRINGARTEN (1980). A double-porosity model was chosen since the early-time data showed features which are characteristic of this model. Geological information also supports the possible existence of a double-porosity environment (e.g. ALEXANDER et al., 1990a). The analysis provided hydraulic conductivity data for both the fracture and the matrix/fill material. The fracture transmissivity averaged about  $2 \cdot 10^{-6}$  m<sup>2</sup>/sec for all boreholes and the fracture hydraulic conductivity was estimated to be  $2 \cdot 10^{-3}$  m/sec based on a fracture aperture of 0.001 m. The matrix conductivity was estimated to be 9 orders of magnitude smaller than the fracture conductivity or  $10^{-12}$  m/sec. The limitations to the double-porosity fracture-flow model is that it cannot be considered a unique solution for the observed responses. Other models may exist which could give an equally viable explanation of the observed responses.

Other phenomena observed during the long-term testing included decreases in the matrix interval pressures. The matrix pressures, however, show a yearly cyclic pattern with lower values occurring in winter. Therefore, it is not possible to relate decreases in the matrix pressure to the long-term pumping. The barometric and earth tide effects were seen to dominate the late-time recovery data. Additional information concerning the long-term hydraulic test is available in GEMPERLE, 1990.

## 6 Conclusions

Exploration and instrumentation work within the GTS has provided a location which is suitable for migration experiments. The location AU96m provides a flow field which is sufficiently stable for migration experiments within a water bearing fracture. This fracture extends far enough to support migration experiments on the intended scale. The transmissivity is in the order of  $10^{-6} - 10^{-7}$  m<sup>2</sup>/sec and allows the set up of a flow field which results in travel times between the boreholes, for conservative tracers, in the order of some hours. The existing boreholes and their instrumentation within an area of about 100 m<sup>2</sup> of the fracture are suitable for tracer experiments in different hydraulic conditions. With this arrangement of boreholes, a "small" field-scale facility, a step up from laboratory-scale experiments, is available for the study of migration processes. The results of concomitant studies of the composition of the groundwater and of the rock/water interactions (BRADBURY, 1989), and model studies of groundwater flow (HERZOG, 1989) corroborate the suitability of the location AU96m for migration experiments. This is especially true for moderately reactive tracers which would require inordinately long times to migrate through a longer flow field.

The purpose of the simple evaluations of the hydraulic tests given here was to provide a basis for the hydraulic model of HERZOG (1989). The results of these tests allow more refined evaluations for enhanced demands.

With the results of the site investigation available, tracer experiments are now under way. These experiments use the non-retarded tracers <sup>82</sup>Br, Uranine and Helium, the only slightly retarded tracers <sup>24</sup>Na, <sup>22</sup>Na and <sup>85</sup>Sr. The purpose of the experiments with the non-retarded tracers is to measure the travel-time distribution of the groundwater. Retarded radionuclides, used in minute concentrations, should yield information about isotope-exchange and other sorption mechanisms (BRADBURY, 1989).

The exploration work at the migration site brought to light several potential problems: 1) the heterogeneity of the fracture with respect to transmissivity and flow channels will make an interpretation of tracer breakthrough data difficult. 2) the high flow velocities with respect to laboratory column experiments may lead to non-equilibrium effects.

## **Acknowledgement**

We thank H.R. Keusen (GEOTEST), M. Bradbury (PSI), R. Gemperle (SOLEXPERTS), W. Drost and H. Behrens (GSF) for cooperation. Thanks also to J. McCort (INTERA), J. Hadermann and F. Herzog (PSI) and W.R. Alexander (Uni Bern) for a careful review of the manuscripts, and C. Degueldre for the “Résumé” in French.

## References

- ABELIN, H. (1986): Migration in a single fracture. An in situ experiment in a natural fracture; PhD thesis, Royal Inst. of Technol., S-100 44 Stockholm, Sweden.
- ALEXANDER, W.R., MCKINLEY, I.G., MACKENZIE, A.B. and SCOTT, R.D. (1990a): Verification of matrix diffusion by means of natural decay series disequilibria in a profile across a water conducting fracture in granitic rock; *Sci. Basis Nucl. Waste Manag.*, XIII (in press).
- ALEXANDER, W.R., MACKENZIE, A.B., SCOTT, R.D. and MCKINLEY, I.G. (1990b): Natural analogue studies in crystalline rock: the influence of water bearing fractures on radionuclide immobilisation in a crystalline rock repository; NAGRA NTB 87-08 (in press), NAGRA, Baden, Switzerland.
- BISCHOFF, K., WOLF, K., HEIMGARTNER, B. (1987): Hydraulische Leitfähigkeit, Porosität und Uranrückhaltung von Kristallin und Mergel; NAGRA NTB-85-42, NAGRA, Baden.
- BOURDET, D. and GRINGARTEN, A.C. (1980): Determination of fissure volume and block size in fractured reservoirs by type-curve analysis; *Sox. Petr. Eng. AIME, SPE* 9293, Dallas, Texas.
- BOUSSINESQ, J. (1904): Recherches théoriques sur l'écoulement des nappes d'eau infiltrées dans le sol et sur le débit des sources; *J. Math. pures et appl.*, 10 (5e série), 5-78, 363-394.
- BRADBURY, M.H. (ed.; 1989): Laboratory investigations in support of the Migration Experiments at the Grimsel Test Site; PSI-Bericht Nr. 28, Paul Scherrer Institut, Villigen, Switzerland/NAGRA NTB 88-23, NAGRA Baden, Switzerland.
- BREDEHOEFT, J.D., and PAPADOPULOS, S.S. (1980): A method for determining the hydraulic properties of tight formations; *Water Resour. Res.*, 16(1), 233-238.
- COOPER, H.H. jr., and C.E. JACOB (1946): A generalized graphical method for evaluating formation constants and summarizing well-field history; *Am. Geophys. Union Trans.*, 27(4), 526-534.

DAVISON, C.C., and GUVANASEN, V. (1985): Hydrogeological characterisation, modelling and monitoring of the site of Canada's underground research laboratory; Abstract in : Proc. Int. Symp. of IAH on "Hydrogeology of Rocks of Low Permeability", Mem. IAH 17(2), 797, Tucson USA.

DEGUELDRE, C., BAEYENS, B., GÖRLICH, W., RIGA, J., VERBIST, J. and STADELMANN, P. (1989): Colloids in water from a subsurface fracture in granitic rock, Grimsel Test Site, Switzerland; *Geochim. Cosmochim. Acta* 53(3), 603-610.

FERRIS, J.G. KNOWLES, D.B., BROWNE, R.H. and STALLMANN, R.W. (1962): Theory of aquifer tests; U.S. Geol. Surv. Water-Supply Pap. 1536-E.

FRICK, U., BÄRTSCHI, P., and HOEHN, E., (1988): Migration investigations. – NAGRA Bull. Spec. Ed. 23-34, NAGRA, Baden, Switzerland.

GELHAR, L.W. and AXNESS, C.L. (1983): Three-dimensional stochastic analysis of macrodispersion in aquifers; *Water Resour.Res.*, 19(1), 161-180.

GEMPERLE, R. (1990): Migration GTS: Test description and first analysis of a 35-day constant-flow test in BOMI 87.009, NAGRA NIB 89-14 (in prep.), NAGRA, Baden, Switzerland.

HADERMANN, J. and HERZOG, F. (1985a): Auswahlkriterien für den Standort eines möglichen Migrationsexperiments im Felslabor Grimsel; EIR-AN-45-85-53, Internal Report, Paul Scherrer Institut, Villigen, Switzerland.

HADERMANN, J. and HERZOG, F. (1985b): Migration experiment at Grimsel: First estimates and calculations; EIR-TM-45-85-45, Internal Report, Paul Scherrer Institut, Villigen, Switzerland.

HADERMANN, J., VON GUNTEN, H.R., McCOMBIE, Ch., and McKINLEY, I.G., (1988): Radionuclide migration in the geosphere. Swiss research in laboratory and field experiments and in model validation; *Rad. Waste Manag. and the Nucl. Fuel Cycle*, 10(1-3), 233-255.

HERZOG, F., (1989), Hydrologic modelling of the Migration Site in the Grimsel Rock Laboratory - The steady state; PSI-Bericht Nr. 35, Paul Scherrer Institut, Villigen, Switzerland/NAGRA NTB 89-16, NAGRA, Baden, Switzerland.

- HOEHN, E. (1986): FLG-MI, Hydraulische Vorabklärungen am Standort AU96m; EIR-TM-44-86-17, Internal Report, Paul Scherrer Institut, Villigen, Switzerland.
- HORNER, D.R. (1951): Pressure build-up in wells; 3rd World Petrol. Congr., 2, 503-521. The Hague, Netherlands.
- INTRAVAL (1987): INTRAVAL Project Proposal; Swedish Nuclear Power Inspectorate, SKI 87-3, Stockholm.
- JACOB, C.E., and LOHMAN, S.W. (1952): Nonsteady flow to a well of a constant drawdown in an extensive aquifer; Am. Geophys. Union Trans., 33, 559-569.
- KEUSEN, H.R. (1989): Rohdatenbericht Geologie, Felslabor Grimsel, 1979 - 1986; NAGRA NIB 87-42, NAGRA, Baden, Switzerland.
- KUSSMAUL, H. and ANTONSEN, O. (1985): Hydrochemische Labormethoden für das NAGRA-Untersuchungsprogramm, NAGRA NTB 85-04, NAGRA, Baden, Switzerland.
- LASSAGNE, D. (1983): Essai de caractérisation du milieu fracturé en massif granitique; Site de Fanay-Augères (Haute-Vienne), Rapp. BRGM 83SGN576 GEG.
- LOHMAN, S.W. (1972): Groundwater hydraulics; U.S. Geol. Survey Prof. Pap. 708, U.S. Government Print. Office, Washington.
- MOSER, H., and RAUERT, H. (1980): Isotopenmethoden in der Hydrologie; Lehrbuch der Hydrogeologie 8, Gebr. Bornträger, Berlin.
- NAGRA (1985): Felslabor Grimsel, Rahmenprogramm und Statusbericht, NAGRA NTB 85-34, NAGRA, Baden, Switzerland.
- NEUZIL, C.E. (1982): On conducting the modified slug test in tight formations; Water Resour. Res., 18(2), 439-441.
- NERETNIEKS, I., ERIKSEN, T. and TÄHTINEN, P. (1982): Tracer movement in a single fissure in granitic rock: some experimental results and their interpretation; Water Resour. Res., 18(4), 849-858.
- SIEGENTHALER, U., SCHOTTERER, U. and OESCHGER, H. (1983): Sauerstoff-18 und Tritium als natürliche Tracer für Grundwasser; Gas-Wasser-Abwasser 63(9), 477-483.

THORNE, P. (1990): Migration GTS: Borehole equipment used for hydrotesting and pilot tracer experiments; NAGRA NIB 89-10 (in prep.), NAGRA, Baden, Switzerland.

WEYER, K.U. (1972): Ermittlung der Grundwassermengen in den Festgesteinen der Mittelgebirge aus Messungen des Trockenwetterabflusses; Geol. Jb. C3, 19-144.

## Appendix A

### Supplement to the chemical characterisation of the groundwaters

A prerequisite for injection – withdrawal (“doublet”) migration experiments is a thorough knowledge of the composition of the in situ, the injection and the mixed groundwaters, as outlined in section 2.3. The composition of the main constituents of the in situ groundwater at the outlet “K” in the tunnel at location AU96m have been described by BRADBURY (1989). The composition of the groundwater does not change significantly over time.

Here, supplementary information on the composition of the in situ and injection groundwaters will be provided. The information includes measurements in boreholes and measurements of trace components such as dissolved gases and isotopes. Groundwater from borehole BOEM 85.012, which is located about 250 m south of AU96m, in the main access tunnel outside the GTS is also presented.

#### 1. Measurements from various boreholes

Since 1987, the major groundwater constituent in boreholes BOMI, outlet “K” and the borehole BOEM 85.012 were analysed on two or three dates. On one or two of the dates, waters were sampled and analysed by PSI, with the methods described in BRADBURY (1989). Apart from that, the anions,  $\text{Cl}^-$ ,  $\text{F}^-$ ,  $\text{NO}_3^-$  and  $\text{SO}_4^{2-}$ , were analysed more recently by standard ion chromatographic techniques. On the first date (October 27, 1987), waters from boreholes BOMI and outlet “K” were sampled and analysed by Institut Fresenius Inc., 6204 Taunusstein-Neuhof, FRG (the groundwater of borehole BOEM 85.012 was analysed earlier). These analyses are given for comparison. The concentration of the main constituents are given in Table A1. As expected, the composition of the groundwaters in the different boreholes BOMI is similar, and similar also to the analyses given in BRADBURY (1989). For most of the parameters the spatial variability was not much greater than the analytical errors ( $\pm 10\%$ ). Some of the analyses of Fresenius deviate significantly from the others (e.g.  $\text{Si}_{\text{tot}}$ ,  $\text{Mg}^{2+}$ ). This table updates the data of BRADBURY (1989).

Table A1 shows that the groundwater of the borehole BOEM 85.012 is similar to that of the BOMI boreholes. The ionic strength and the pH are somewhat lower;  $\text{Cl}^-$  and  $\text{F}^-$ -concentrations are considerably lower in the BOEM groundwater. The cations most

relevant for migration experiments,  $\text{Na}^+$ ,  $\text{Ca}^{2+}$  and  $\text{Sr}^{2+}$ , vary by a factor of about two;  $\text{K}^+$  and  $\text{Mg}^{2+}$  vary considerably more.

Some of the trace components analysed by Fresenius in BOMI and BOEM groundwaters and shown in Table A2 are of particular interest for migration experiments. The slight smell from the groundwaters of  $\text{H}_2\text{S}$ ,  $\text{Fe}^{2+}$ —concentrations below the detection limit of 0.02 ppm, trace amounts of  $\text{Mn}^{2+}$ , and negative mV values for the redox potential, all indicate slightly reducing conditions. In combination with the low ionic strength of about 1 mM the results showed that the redox equilibria of these groundwaters are very difficult to model.  $\text{Li}^+$ ,  $\text{Ba}^{2+}$ , Al and  $\text{Br}^-$  species are present in trace amounts, but do not contribute to the ion balance.

Table A1: Chemical composition of groundwaters in boreholes and in outlet "K". P = PSI; F = Inst. Fresenius

Borehole	BOMI 86.004		BOMI 86.005		BOMI 86.006		BOMI 86.009		outlet "K"			BOEM 85.012		
	F	P	F	P	P	P	F	P	F	P	P	F	P	P
Date	27.10.87	21.06.88	27.10.87	21.06.88	21.06.88	20.07.88	27.10.87	21.06.88	27.10.87	21.06.88	20.07.88	01.07.86	21.06.88	20.07.88
pH	9.62	-	9.40	-	-	8.96	9.59	-	9.56	-	9.12	8.90	8.90	-
LF $\mu\text{S cm}^{-1}$	108	-	108	-	-	90.0	108	-	106	-	96.9	69	75	-
Alk mM	0.43	0.41	0.42	0.42	0.40	0.45	0.42	0.40	0.42	0.40	0.42	-	0.60	0.54
K ppm	0.14	0.175	0.16	0.191	0.147	0.333	0.22	0.144	0.14	0.120	0.134	0.91	0.94	1.02
Na "	16	16.9	16	16.9	16.8	(?) 12.0	16	16.7	16	15.5	15.5	5.7	6.04	5.99
Ca "	5.7	5.62	5.7	5.81	5.72	6.53	5.6	5.69	5.7	5.59	5.58	8.6	8.86	9.12
Mg "	0.049	0.013	0.049	0.014	0.009	0.030	0.044	0.009	0.049	0.012	0.011	0.06	0.094	0.106
Sr "	0.15	0.179	0.17	0.184	0.182	0.215	0.18	0.183	0.17	0.175	0.169	0.32	0.304	0.332
Si <sub>tot</sub> "	12	-	12	-	-	5.34	12	-	12	-	5.75	12.2	4.60	-
F "	6.0	6.05	6.1	5.75	5.95	4.70	6.1	5.95	6.0	5.45	6.0	0.87	1.48	1.4
Cl "	5.5	5.45	6.1	6.05	5.25	3.60	5.5	5.35	5.0	4.0	4.7	0.20	0.21	0.29
NO <sub>3</sub> "	<0.3	0.009	<0.3	0.04	0.008	0.07	<0.3	<0.003	<0.3	<0.003	0.01	<0.3	<0.003	0.003
SO <sub>4</sub> "	5.6	-	5.2	-	-	5.0	5.5	-	5.6	-	6.5	4.9	4.2	-
Al "	0.044	-	0.020	-	-	-	0.012	-	0.047	-	-	0.017	-	-
Ca/Na "	0.36	0.33	0.36	0.34	0.34	(?) 0.54	0.35	0.34	0.36	0.36	0.36	1.51	1.47	1.52
F/Cl "	1.09	1.11	1.00	0.95	1.13	1.31	1.09	1.11	1.20	1.36	1.28	4.35	7.05	4.83

Table A2: Trace constituents of groundwaters (analyses: Inst. Fresenius)

Borehole: Date: n = Number of analyses	BOMI 27.10.87 n = 4	BOEM 85.012 01.07.86 n = 1
T (°C)	12.6 ± 0.26	10.4
Eh (mV)	-382 ± 17	-50
DOC (ppm)	0.7 ± 14	1.3
Li (ppm)	0.09 ± 0.01	0.02
Ba (ppm)	< 0.005	0.04
Mn <sup>2+</sup> (ppm)	0.003 ± 0.001	0.013
Fe <sup>2+</sup> (ppm)	< 0.02	< 0.02
Br <sup>-</sup> (ppm)	0.05 ± 0.003	< 0.05
Al (ppm)	0.03 ± 0.02	0.017

## 2. Gas content and isotope measurements

This section compiles results of measurements of a) dissolved gases; b) uranium concentrations; and c) environmental isotopes. It complements the results reported by BRADBURY (1989).

The gas contents of the various groundwaters, shown in Table A3, do not vary much. The low concentrations of CO<sub>2</sub> and O<sub>2</sub> are of particular interest for the chemical modelling. It was interesting to note the concentrations of H<sub>2</sub>S to be below the detection limit, although the gas could be smelled. The concentrations above atmospheric probably result from the dissolution of U from minerals of the rock matrix, see below.

Concentrations of total dissolved uranium in the flowing groundwaters were measured on Sept. 2, 1986, at the outlet "K" and in the BOEM groundwater, and analysed with the method reported in KUSSMAUL and ANTONSEN (1985). Both analyses resulted in concentrations of 0.09 ppb. U in the solid phase varies from 5 – 8 ppm in the AU96m granodiorite to a maximum of 12 ppm in the protomylonitic fracture fill (ALEXANDER et al., 1990a). Chemical leaching experiments on both materials indicate that the U is tightly bound and unlikely to be easily accessible to percolating waters (ALEXANDER et al., 1990b).

Table A3: Dissolved gases (mg/kg; CO<sub>2</sub>, mmol/kg)

Date	Volume (cm <sup>3</sup> /kg)	Location	H <sub>2</sub>	He	N <sub>2</sub>	O <sub>2</sub>	Ar	H <sub>2</sub> S <sup>1)</sup>	CH <sub>4</sub>	CO <sub>2</sub>
27.06..88	17.4	BOEM 85.012	$6 \cdot 10^{-4}$	n.n.	21.2	0.035	0.73	–	n.n.	0.002
29.10.87	–	outlet “K”	$10^{-4}$	n.n.	19.3	0.03	0.70	n.n.	Sp	$<6 \cdot 10^{-4}$
29.10.87	–	BOMI 87.009	$9 \cdot 10^{-4}$	$4 \cdot 10^{-4}$	24.6	0.003	0.79	0.002	n.n.	n.n.
02.09.86	16.7	outlet “K”	$5 \cdot 10^{-4}$	$6 \cdot 10^{-4}$	20.3	0.03	0.72	n.n.	n.n.	$<7 \cdot 10^{-4}$
02.09.86	18.1	BOEM 85.012	$3 \cdot 10^{-4}$	$<5 \cdot 10^{-4}$	22.0	$<5 \cdot 10^{-4}$	0.73	$<10^{-2}$	$<5 \cdot 10^{-4}$	n.n.

<sup>1)</sup> slight smell

n.n. = below detection limit

Tritium,  $^2\text{H}$  and  $^{18}\text{O}$  were measured by Gesellschaft für Strahlen- und Umweltforschung (GSF), Institut für Hydrologie, Neuherberg-München, FRG, at various locations in the GTS, among them location AU96m. At this location, the concentrations found were below 1 TU (in 1983 and 1984). In 1986, 12 samples showed an average value of  $2.3 \pm 0.7$  TU. From this we concluded that mean travel times of the groundwater from the ground surface to the AU96m fracture are above 30 years (e.g. MOSER and RAUERT, 1980). Such a long period for an average linear vertical flow distance from the ground surface to the tunnel of about 400 m is in discrepancy with the results of section 2.3, where the transport velocity for the dissolved oxygen from borehole BOMI 87.008 to the outlet "K" was estimated to be in the order of a few meters per hour. Similarly, high flow velocities were found during tracer experiments. The latter travel-time estimates were, however, made under disturbed conditions with steep superimposed hydraulic gradients. A verification with tritium, of the assumption that the groundwater is older than 30 years is now increasingly difficult. The isotope, which originated from bomb tests in the fifties, has decayed and reached almost background activities in surface waters.

Twelve samples of the groundwater at location AU96m were analysed for  $\delta^2\text{H}$  and  $\delta^{18}\text{O}$ . They exhibited values of about  $-98 \pm 1\text{‰}$  and  $-13.72 \pm 0.05\text{‰}$ , respectively. The data fit well into a straight-line correlation of the two parameters with other groundwaters from the GTS. A comparison of the measurements at location AU96m with values of groundwaters from nearby alpine catchment areas (SIEGENTHALER et al., 1983) revealed an average altitude for seepage of about 2000 m.a.s.l. This is almost in accordance with the altitude of the local ground surface of 2200 – 2400 m.a.s.l.

Fourteen measurements of Radon-222 in the boreholes BOMI in 1987, at steady flow conditions, revealed concentrations of  $23 \pm 2.7$  Bq/L, and 13 measurements at the outlet "K" revealed concentrations of  $17 \pm 2.8$  Bq/L. We believed that the groundwater at the outlet "K" is subject to some outgassing, which would explain the lower radon values. The radon concentrations did not vary during a short experiment in borehole BOMI 87.008, when the stagnant water was sampled several times immediately after opening the borehole until the packed off volume was flushed about three times.

## Appendix B

### Compilation of Transmissivity and Storage-Coefficient Calculations

Table B1: Transmissivity and Storage Coefficient of Constant-Drawdown Tests (E-06 = 10<sup>-6</sup>)

Tested Borehole	Test Date	Observ. Borehole	Calculated Transmissivity (m <sup>2</sup> /sec)			Calculated Storage Coefficient
			Flow Period	Steady State	Recovery	
86.004	06-11-86	****	1.3E-06	3.7E-07	1.9E-06	
		86.005	2.0E-06	—	—	
	08-12-87	****	1.6E-06	4.3E-07	3-15E-07	
		86.005	1.7E-06	3.3E-06	2.0E-06	3.2E-07
		87.006	2.2E-06	2.3E-06	—	1.7E-07
		87.008	3.2E-06	1.1E-05	—	4.2E-05
		87.009	2.2E-06	2.2E-06	—	2.8E-07
		87.010	2.7E-06	9.6E-06	1.8E-06	1.4E-05
C	2.9E-05	9.5E-05	—	2.9E-04		
86.005	16-12-86	****	4.2E-08	1.0E-08	8-20E-08	—
	10-12-87	****	4.1E-08	2.1E-08	3-67E-09	
87.006	26-08-87	****	1.1E-06	2.0E-07	2.0E-06	
		86.004	2.1E-06	2.7E-06	1.7E-06	5.4E-07
		86.005	2.1E-06	3.6E-06	1.7E-06	4.3E-07
		87.008	1.7E-06	6.2E-06	1.5E-06	1.4E-07
		87.009	2.1E-06	1.8E-06	1.6E-06	2.6E-06
		87.010	1.6E-06	5.9E-06	1.4E-06	2.7E-05
		C	1.8E-06	4.1E-06	2.7E-06	1.1E-03
87.008	28-08-87	****	7-24E-07	5.0E-07	4-9E-07	
		86.004	3.8E-06	9.3E-06	1.6E-06	2.5E-05
		86.005	3.5E-06	7.9E-06	1.6E-06	2.1E-05
		87.006	4.0E-06	6.9E-06	1.5E-06	1.1E-04
		87.009	3.9E-06	8.2E-06	1.7E-06	2.8E-05
		87.010	1-6E-06	1.3E-06	9-37E-07	2.4E-06
		C	8.7E-07	1.6E-06	6.7E-07	1.4E-04
87.009	27-08-87	****	4.4E-06	9.3E-07	4-22E-07	
		86.004	2.4E-06	2.0E-06	9-20E-06	3.5E-08
		86.005	2.3E-06	2.9E-06	9-20E-06	4.6E-08
		87.006	4.2E-06	1.1E-06	7-20E-07	—
		87.008	2.3E-06	5.8E-06	2-3E-06	5.1E-05
		87.010	2.1E-06	6.2E-06	1-9E-06	1.4E-05
		C	2.8E-06	7.3E-06	2-10E-06	3.8E-05
87.010	31-08-87	****	—	5.4E-07	3-49E-07	
		86.004	3.0E-06	1.1E-05	3.2E-06	7.2E-06
		86.005	—	7.8E-06	—	—
		87.006	2.8E-06	8.1E-06	2.9E-06	2.1E-05
		87.008	7 - 16E-07	1.0E-06	3.7E-07	—
		87.009	3.0E-06	9.6E-06	3.0E-06	1.4E-05
		C	8 - 21E-07	1.2E-06	5.0E-07	—

\*\*\*\* = Single Borehole Analysis

Tabelle B2: Transmissivity and storage coefficient of Constant-Discharge Tests ( $E-06 = 10^{-6}$ )

Tested Borehole	Test Date	Observ. Borehole	Calculated Transmissivity ( $m^2/sec$ )			Calculated Storage Coefficient
			Flow Period	Steady State	Recovery	
86.004	09-12-87	****	1.4E-06	5.6E-07	9-16E-07	
		86.005	1.2E-06	2.5E-06	1-2E-06	6.6E-07
		86.006	1.2E-06	1.8E-06	1.8E-06	2.7E-06
		87.008	2.7E-06	8.4E-06	2.6E-06	4.3E-05
		87.009	1.2E-06	1.7E-06	1.6E-06	4.9E-06
		87.010	2.3E-06	7.4E-06	2.0E-06	1.4E-05
		C	2.5E-05	2.3E-05	2.2E-05	2.3E-04
86.004	10-12-87	****	1.4E-06	4.4E-07	1.7E-06	
		86.005	1.8E-06	3.4E-06	1-3E-06	1.9E-07
		87.006	1.8E-06	2.5E-06	1-2E-06	4.3E-07
		87.008	2.5E-06	1.2E-05	2.1E-06	4.9E-05
		87.009	1.8E-06	2.4E-06	1-2E-06	7.9E-07
		87.010	2.3E-06	1.0E-05	2.0E-06	1.5E-05
		C	2.3E-05	1.2E-04	1.8E-05	3.2E-04
87.009	01-09-87	****	1.9E-06	1.1E-06	—	
		86.004	1.9E-06	2.2E-06	—	1.2E-06
		86.005	2.0E-06	3.2E-06	—	3.1E-07
		87.006	1.9E-06	1.3E-06	—	4.7E-07
		87.008	3.0E-06	9.6E-06	—	1.4E-05
		87.010	2.7E-06	8.3E-06	—	2.7E-05
		C	3.5E-06	1.0E-05	—	9.1E-05

\*\*\*\* = Single Borehole Analysis